# Neptune and Company Inc.

June 1, 2011 Report for EnergySolutions

Clive DU PA Model, version 1

## Appendix 13

Deep Time Assessment

# Deep Time Assessment for the Clive DU PA

30 May 2011

Prepared by

Neptune and Company, Inc.

This page is intentionally blank, aside from this statement.

# CONTENTS

# FIGURES

# TABLES

# 1.0 Deep Time Scenarios Distribution Summary

The following is a brief summary of input values used parameters employed in the deep time[1] scenarios component of the Clive Performance Assessment (PA) model that is the subject of this white paper.

For distributions, the following notation is used:

- LN( *GM*, *GSD*, [*min*, *max*] ) represents a log-normal distribution with geometric mean GM and geometric standard deviation GSD, and optional *min* and *max*, and
- Beta( μ, σ, *min*, *max* ) represents a generalized beta distribution with mean μ, standard deviation σ, minimum *min*, and maximum *max*.

**Table 1. Summary of distributions for the Deep Time Scenarios container.**

| Model Parameter | Value or Distribution | Units | Reference / Comments |
|---|---|---|---|
| LargeLakeStart | LN( GM=14000, GSD=1.2, min=0, max=50000 ) | yr | See Section 6.1 |
| LargeLakeEnd | LN( GM=6000, GSD=1.2, min=0, max=50000 ) | yr | See Section 6.1 |
| LargeLakeSedimentationRate | LN( GM=0.00012, GSD=1.2 ) | m/yr | See Section 6.3 |
| IntermediateLakeDuration | LN( GM=500, GSD=1.5, min=0, max=2500 ) | yr | See Section 6.2 |
| IntermediateLake SedimentAmount | LN( GM=2.82, GSD=1.71 ) | m | See Section 6.3 |
| SiteDispersalArea | LN( GM= VolumeAboveGrade / 0.1 m, GSD=1.5, min= VolumeAboveGrade / 1 m, max=Large[1]) | $km^2$ | See Section 6.4 |
| IntermediateLakeDepth | beta( μ=30, σ=18, min = 0, max = 100 ) | m | See Section 6.5 |
| LargeLakeDepth | beta( μ=150, σ=20, min = 100, max = 200 ) | m | See Section 6.5 |

[1]"Large" is an arbitrarily large number defined in the Clive DU PA Model as 1E+30.

# 2.0 Deep Time Scenarios Overview

There are two major components to the Clive depleted uranium (DU) Performance Assessment (PA) model. The first addresses quantitative dose assessment for 10,000 years and is based on projections of current societal conditions into the future, which also assumes no substantial change in climatic conditions. The second addresses simulations until the time of peak radioactivity. For this PA, peak radioactivity associated with radon production from DU, occurs

1 For the purpose of this white paper, deep time refers to the period between 10 thousand years to 2.1 million years

at about 2.1 My. The time frame of this component requires consideration of climatic changes based on the scientific literature that have occurred on approximately 100 ky cycles for more than 1 My. These cycles include periods of extensive glaciation and inter-glacial periods (Figure 1). The planet is currently in an inter-glacial period. In effect, the 10 ky model is projected under inter-glacial conditions, and the deep time model includes an evaluation of the effect on DU disposal in the Class A South embankment of future 100 ky glacial cycles for the next 2.1 My. The focus of this paper is the deep time model.

The objective of the deep time scenarios submodel in the GoldSim (GTG, 2011) PA model is to assess the potential impact of glacial epoch pluvial lake events on the overall DU waste embankment from 10 ky through 2.1 My post-closure. A pluvial lake is a consequence of periods of extensive glaciation, and results from low evaporation, increased cloud cover, increased albedo, and increased precipitation in landlocked areas.

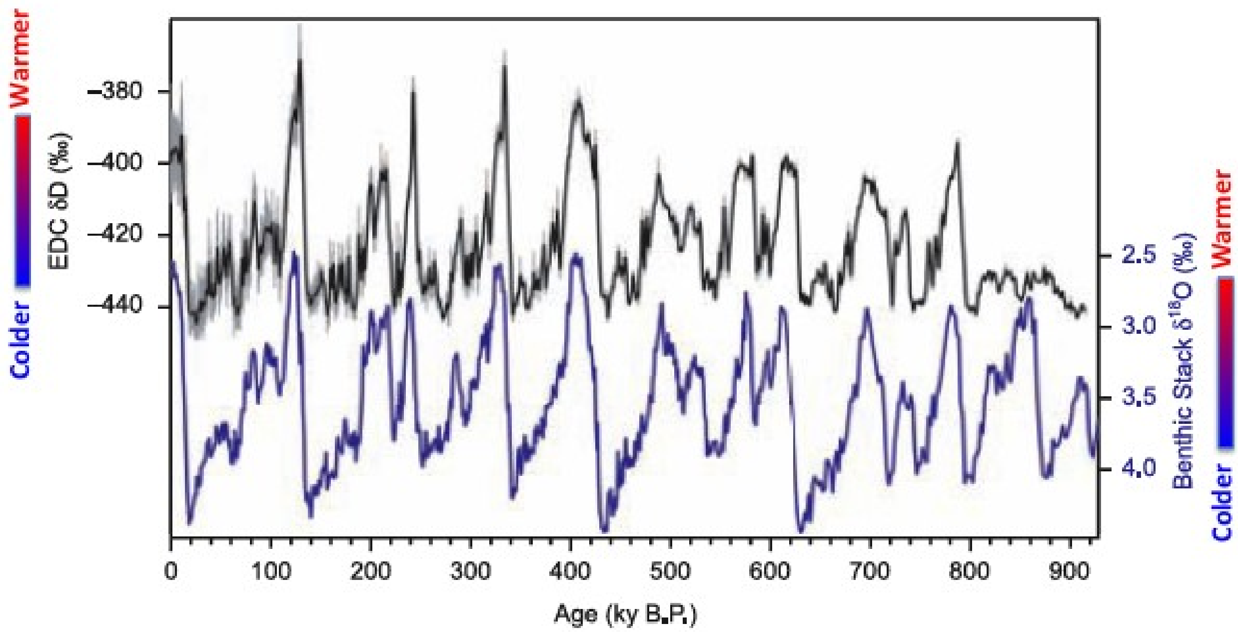


**Figure 1. Comparison of delta deuterium (black line) from the European Project for Ice Coring in Antarctica (EPICA) Dome C ice core and benthic (marine) oxygen-18 record (blue line) for the past 900 ky [reproduced from Jouzel et al. (2007)].** Note that the two records are correlated for about the past 800 ky.[2]

The deep time evaluation focuses on potential releases of radioactivity following a series of lake events caused by glacial cycles (Figure 1). The approximate 100 ky glacial cycles can be easily discerned in Figure 1. The current inter-glacial period is shown on the left edge of the figure. The last ice age finished between 12 ky and 20 ky ago. Around the last glacial maxiumum (represented as a trough on the far-left side of Figure 1), Lake Bonneville reached its maximum extent. The ice core data and the benthic marine isotope data show very similar patterns for the

2 Both time series have been used as proxies for representing major shifts (glacial and interglacial shifts, represented by the temperature gradient on the y-axes) in past climate.

past 800 ky. These 100 ky cycles are used as the basis for modeling the return and recurrence of lake events in the Bonneville Basin.

The approach to deep time modeling is briefly described in the *Conceptual Site Model for Disposal of Depleted Uranium at the Clive Facility* (Neptune, 2011a). The model is developed further in this paper, including more detailed conceptual model development, model structuring and model specification based on available data, scientific literature, and expert opinion.

For the deep time evaluation, the PA model provides an assessment of plausible future consequences of present-day disposal of DU waste to the environment. Doses to potential human receptors are not calculated. However, projected concentrations of radioactive species are tracked in both lake water and lake sediments. Although the 100 ky glacial patterns can be used as a basis for modeling lake recurrence, specific temporal information available for assessing the long-term behavior of the DU waste disposal system and the area surrounding the Clive site is highly uncertain. That is, although large lakes are expected to return, the exact timing is uncertain. However, the exact timing is not important. What is important is that the model allows for periodic recurrence of large lakes similar to those that have occurred in the past which could inundate the Clive area in the future. Given this ability, the impact of large lakes on the disposal system can then be evaluated.

Thus the deep time model constructed should be regarded as conceptual and stylized. The intent is to present a picture of what the future might hold for the DU waste disposal embankment, rather than to provide a quantitative, temporally specific, prediction of future conditions, or an assessment of exposure or dose to human receptors who might or might not exist long into the future. The type of glacial climate change envisioned in the deep time model will probably have wide-reaching consequences for the planet, that are far beyond the scope of a PA for disposal of radioactive waste.

The focus of the deep time evaluation is return of large lakes in the Bonneville Basin. Since climatic cycles are considered very likely, in which case the deep time model evaluates the consequences of the return of large lakes. Other less likely geologic events could also occur in the next 2.1 My. Events such as meteor strikes, and volcanic activity such as Yellowstone could also be considered. However, events other than the cyclic return of large lakes are not considered further in this model because their likelihood is small, and their consequences are likely to be much greater and far reaching for human civilization.

The background sections provide a detailed overview of past climatic conditions that have been linked to the formation of pluvial lake events in the Bonneville Basin, which is the large drainage basin in Utah that has been subject to pluvial lake events in the past. For example, the Great Salt Lake is a remnant of Lake Bonneville, the pluvial lake that existed at the last glacial maximum. The background sections are then followed by a presentation of the conceptual site model and the specific functions and parameters implemented in the deep time container in the GoldSim PA model.

# 3.0 Background on Pluvial Lake Formation in the Bonneville Basin

## 3.1 Long-term Climate

Large-scale climatic fluctuations over the last 2.6 My (the beginning of the Quaternary Period in geologic time) have been studied extensively in order to understand the mechanisms underlying those changes (Hays et al., 1976, Berger, 1988, Paillard, 2001, Berger and Loutre, 2002). These climatic signals have been observed in marine sediments (Lisiekcki and Raymo, 2005), land records (Oviatt et al., 1999), and ice cores (Jouzel et al., 2007). These large-scale fluctuations in climate have resulted in glacial and interglacial cycles, which have waxed and waned throughout the Quaternary Period. The causes of the onset of the last major Northern Hemisphere glacial cycles 2.6 My ago remain uncertain, but several studies suggest that the closing of the Isthmus of Panama caused a marked reorganization of ocean circulation patterns that resulted in continental glaciation (Haug and Tiedemann, 1998, Driscoll and Haug, 1998). Future glacial events are likely to be caused by a combination of the Earth's orbital parameters as well as increases in freshwater inputs to the world's oceans resulting in a disruption to the ocean's thermohaline circulation (Driscoll and Haug, 1998).

Changes in the periodicity of glacial cycles have been linked to variations in Earth's orbit around the Sun. These variations were described by Milankovitch theory and are based on changes that occur due to the eccentricity (i.e., orbital shape) of Earth's orbit every 100 ky, the obliquity (i.e., axial tilt) of Earth's axis every 41 ky, and the precession of the equinoxes (or solstices) (i.e., wobbling of the Earth on its axis) every 21 ky (Berger, 1988). For the first 2 My of the Pleistocene (the first major Epoch of the Quaternary Period), Northern Hemispheric glacial cycles occurred every 41 ky, while the last million years have indicated glacial cycles occurring every 100 ky, with strong cyclicity in solar radiation every 23 ky (Berger and Loutre, 2002; Paillard, 2006). The shift from shorter to longer cycles is one of the greatest uncertainties associated with utilizing the Milankovitch orbital theory alone to explain the onset of glacial cycles (Paillard, 2006).

The evaluation by Hays et al. (1976), who analyzed changes in the isotopic Oxygen-18 ($\delta^{18}O$) composition of deep-sea sediment cores, suggest that major climatic changes have followed both the variations in obliquity and precession through their impact on planetary insolation (i.e., the measure of solar radiation energy received on a given surface area in a given time). In its most common form, Oxygen in composed of 8 protons and 8 neutrons (giving it an atomic weight of 16). This is know as a "light" oxygen. It is called "light" because a small fraction of oxygen atoms have 2 extra neutrons and a resulting atomic weight of 18 ($O^{18}$), which is then known as "heavy" oxygen. $O^{18}$ is a rare form and is found in only about 1 in 500 atoms of oxygen. The ratio of these two oxygen isotopes has changed over the ages and these changes are a proxy to changing climate that have been used in both ice cores from glaciers and ice caps and cores of deep sea sediments. Thus, variations in $\delta^{18}O$ reflect changes in oceanic isotopic composition caused by the waxing and waning of Northern Hemispheric ice sheets, and are thus used as a proxy for previous changes in climate (cf. Figure 1).

Slightly different external forcing and internal feedback mechanisms can lead to a wide range of responses in terms of the causes of glacial-interglacial cycles. The collection of longer ice core records, such as the European Project for Ice Coring in Antarctica (EPICA) Dome C core located in Antarctica, has highlighted the clear distinctions between different interglacial-glacial cycles (Jouzel et al., 2007). For example, the last glacial period resulted in the presentation of Lake Bonneville, perhaps the largest glacial lake that has occurred in the Bonneville Basin. However, of the seven most recent 100 ky glacial cycles, it is estimated that only four of them presented very large lakes in the Bonneville Basin. Variation in climatic conditions appears to be sufficient that large differences have occurred in each of the past 100 ky cycles. At the present time, the EPICA Dome C core is the longest (in duration) Antarctic ice core record available, covering the last 800 ky (Jouzel et al., 2007).

Various studies highlight the importance of past atmospheric composition in the dynamics of glaciations across the Northern Hemisphere, in addition to the insolation due to orbital influences (Masson-Delmotte et al., 2010; Clark et al., 2009; Paillard, 2006). Carbon dioxide ($CO_2$) is a well-known influence on the atmospheric 'greenhouse effect' (i.e. warming due to trapping of solar heat), and is a globally well-mixed gas in the atmosphere due to its long lifetime. Therefore, measurements of this gas that are made in Antarctic ice are globally representative and provide long-term data that are important for understanding past climatic changes. Direct measurement of $CO_2$ trapped in the EPICA Dome C core indicates that atmospheric $CO_2$ concentrations decreased during glacial periods due to greater storage in the deep ocean, thereby causing cooler temperatures from a reduction of the atmosphere's greenhouse effect (EPICA, 2004). Warmer temperatures resulting from elevated concentrations of $CO_2$ that is released from the ocean contribute to further warming and could support hypotheses of rapid wasting at the end of glacial events (Hays et al., 1976). Earlier interglacial events (prior to 420 ky), however, are thought to have been cooler than the most recent interglacial events (since 420 ky) (Masson-Delmotte et al., 2010).

Berger and Loutre (2002) conducted simulations including orbital forcing coupled with insolation and $CO_2$ variations over the next 100 ky. Their results indicated that the current interglacial period could last another 50 ky with the next glacial maximum occurring about 100 ky from now. The scientific record (cf. Figure 1) supports variability across the 100 ky glacial cycles. Berger and Loutre (2002) effectively indicate that the current 100 ky cycle will not be as glacially intense as some of the previous cycles. They also quote J. Murray Mitchell (Kukla et al, 1972, p. 436) who predicts that "The net impact of human activities on climate of the future decades and centuries is quite likely to be one of warming and therefore favorable to the perpetuation of the present interglacial". Archer and Ganopolski (2005) conducted simulations that predict that a massive carbon release from fossil fuel or methane hydrate deposits could prevent glaciation for the next 500 ky. The potential impact of anthropogenic $CO_2$ (as opposed to natural sources) is controversial and subject to a large degree of uncertainty, and is not addressed further in this modeling effort. Although human influences might extend the current inter-glacial period, this potential effect is not considered in the deep time model because orbital forcing is expected to dominate further into this glacial cycle.

Berger and Loutre (2002) also report that future increases in atmospheric $CO_2$ from anthropogenic activity along with small insolation variations could result in a transition between the Quaternary and the next geologic period due to the potential wasting of the Greenland and west Antarctic Ice Sheets. However this would also result in increased freshwater inputs to the oceans and could cause a shift toward a colder climate and the next glacial age (Driscoll and Haug, 1998). Given the uncertainties involved in these speculations, the deep time model focuses on stylized projection of the past 800 ky of 100 ky glacial cycles.

Other gases, such as deuterium, have also been measured in the EPICA Dome C core. Jouzel et al. (2007) assembled a high-resolution deuterium profile from the EPICA Dome C core and used these measurements to extend the climate record back to 800 ky ago (see Figure 1). These data indicate that a 100 ky periodicity primarily dominates the temperature record, however the record also indicates that a strong obliquity (40-41 ky) component exists and increases when going from past to present. Jouzel et al. (2007) also indicate that in general, systematic millennial-scale changes are related to North Atlantic deep water formation (influenced by fresh water inputs and sea ice formation), which is shown for the last glacial cycle and suggested for previous glacial periods.

The following sub-sections present an overall background on past events in the Bonneville Basin that are driven by major shifts in climatic regime that are presumed to occur in the future (10 ky to 2.1 My).

## 3.2 Deep Lake Cycles

The Bonneville Basin is the largest drainage basin in the Great Basin of the Western US. It is a hydrologically closed basin that covers an area greater than 134,000 $km^2$, and has previously been occupied by deep pluvial lakes. Pluvial lakes typically form when warm air from arid regions meets chilled air from glaciers, creating cloudy, cool, rainy weather beyond the terminus of the glacier. The increase in rainfall and moisture can fill the drainage basin, forming a lake. This kind of humid climate was evident during the last glacial period in North America, and resulted in more precipitation than evaporation, hence the rise of Lake Bonneville.

Various studies have investigated previous lake cycles in the Bonneville Basin (Table 2; Oviatt et al., 1999; Link et al., 1999). Some of these studies focus on the analysis of sediment cores, which are used to help understand previous lake levels as well as establish the approximate age of previous lake cycles (e.g., Oviatt et al., 1999). Oviatt et al. (1999) analyzed hydrolysate amino acid enantiomers for aspartic acid, which is abundant in ostrocode protein. Ostracodes are small crustaceans that are useful indicators of paleo-environments because of their widespread occurrence and because they are easily preserved. Oviatt et al. (1999) indicate that ostracodes are highly sensitive to water salinity. Therefore, portions of sediment cores that contain ostracodes indicate fresher, and hence probably deeper, lake conditions than the modern Great Salt Lake (Oviatt et al., 1999).

To establish the approximate timing of previous lake cycles, Oviatt et al. (1999) examined sediments from the Burmester sediment core and suggested that a total of four deep-lake cycles occurred during the past 780 ky (Table 2). They found that the four lake cycles correlated with marine $\delta^{18}O$ stages 2 (Bonneville lake cycle: ~24-12 ky), 6 (Little Valley lake cycle: ~186-128 ky), 12 (Pokes Point lake cycle: ~478-423 ky), and 16 (Lava Creek lake cycle: ~659-620 ky).

Oxygen isotope stages are alternating warm and cool periods in the Earth's paleoclimate which are deduced from oxygen isotope data (Figure 2). These correlations suggest that large pluvial lake formation in the Bonneville Basin occurred in the past only during the most extensive Northern Hemisphere glaciations. These extensive glaciations are suggested to have been controlled by the mean position of storm tracks throughout the Pleistocene, which were in turn controlled by the size and shape of the ice sheets (Oviatt, 1997; Asmerom et al., 2010). In addition to these large lake cycles, a smaller cycle known as the Cutler Dam cycle occurred between 80-40 ky (Link et al., 1999).

**Table 2. Lake cycles in the Bonneville Basin during the last 700 ky.[3]**

| Lake Cycle | Approximate Age* | Maximum Elevation | Lake level control |
|---|---|---|---|
| Great Salt Lake (current level) | present | 1284 m (4212 ft) in 1873 | Inter-glacial climate; human intervention |
| Bonneville (Gilbert Shoreline) | 12.9-11.2 ka | 1295 m (4250 ft) | Beginning of inter-glacial climate; possible regressive phase of Lake Bonneville; possible association with the Younger Dryas period |
| Bonneville (Provo Shoreline) | 17.4-15.0 ka | 1445 m (4740 ft) | Glacial climate; new threshold at Zenda near Red Rock Pass, Idaho (natural dam collapse) |
| Bonneville (Bonneville Shoreline) | 18.3-17.4 ka | 1552 m (5090 ft) | Glacial climate; threshold at Zenda near Red Rock Pass, Idaho |
| Bonneville Transgression | ~30-18.3 ka | | Glacial climate |
| Bonneville (Stansbury Shoreline) | 26–24 ka | 1372 m (4500 ft) | Glacial climate; transgressive phase of Lake Bonneville |
| Cutler Dam | ~80–40 ka | < 1380 m (< 4525 ft) | Glacial climate |
| Little Valley | ~128–186 ka | 1490 m (4887 ft) | Glacial climate |
| Pokes Point | 417–478 ka | 1428 m (4684 ft) | Glacial climate |
| Lava Creek | ~620–659 ka | 1420 m (4658 ft) | Glacial climate |

*Approximate ages derived from Currey, et al. (1984) Link et al. (1999) and Oviatt et al. (1999). Bonneville cycle approximate age presented as calibrated years.
Elevations are not corrected for isostatic variations

3 Note the various levels of the last major lake cycle, Lake Bonneville.

Lake Bonneville is the last major deep lake cycle that took place in the Bonneville Basin and is widely described in the literature (Hart et al., 2004; Oviatt and Nash, 1989; Oviatt et al., 1994; 1999). Lake Bonneville was a pluvial lake that began forming approximately 28-30 thousand years before present (ky BP), forming various shorelines throughout its existence and covering over 51,000 $km^2$ at its highest level (Matsurba and Howard, 2009). The high-stand (i.e., the highest level reached) of the lake at the Zenda threshold (1,552 m), located north of Red Rock Pass, occurred approximately 18.3-17.4 ky BP. The high-stand of the lake was followed by an abrupt drop in lake level due to the catastrophic failure of a natural dam composed of unconsolidated material at approximately 17.4 ky BP. As a result of this flood, the lake dropped to a level of 1,445 m, called the Provo level. The Provo level is the maximum level that any future deep lake can reach. The lake regressed rapidly during the last deglaciation, then increased again to form the Gilbert shoreline between 11.2-12.9 ky BP which coincided with the Younger Dryas global cooling event (Oviatt et al., 2005). The lake then receded to levels of the current Great Salt Lake at approximately 10 ky BP for the remainder of the Holocene.

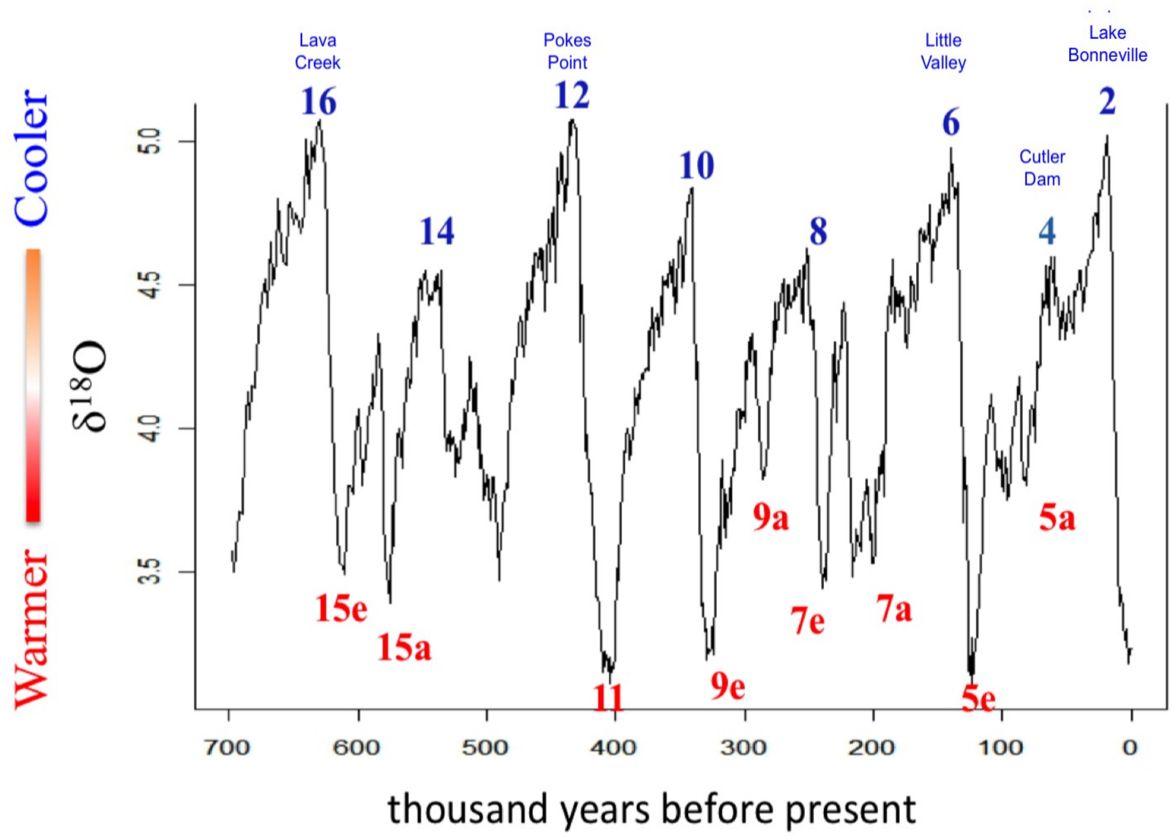


**Figure 2. Benthic oxygen isotope record for the last 700,000 years (Lisiecki and Raymo, 2005).**[4]

4 Red (warm periods) and blue (cool periods) numbers correspond to marine isotope stages based on Lisiecki and Raymo (2005). Lake stages identified by Oviatt et al. (1999) are also included in blue text.

Glacial cycles can be discerned in Figure 2 by considering each cycle from the beginning of the inter-glacial period and ending each cycle at the peaks that correspond to large lake occurrence. Using this approach, the current glacial cycle started around 12 ky ago, Lake Bonneville occurred at the end of the last complete cycle, and Cutler Dam occurred in the middle of the last 100 ky cycle. The previous 100 ky cycle resulted in Little Valley. Pokes Point occurred five cycles ago, and Lava Creek 7 cycles ago. These large lakes have been identified in sediment cores and in shorelines around the Bonneville Basin. However, it is likely that many more shallower lakes have also occurred in each glacial period, but the shorelines have been destroyed by later lakes. In addition, sedimentation in the Bonneville Basin is caused by several factors including air dispersion in inter-glacial periods, and both terrigenous and biotic sedimentation when lakes are formed in glacial periods. In addition, sedimentation in the Bonneville Basin depends on location within the basin, which determines such things as the presence or absence of river input, wave energy, sediment availability on piedmonts, water chemistry, biological activity, and slope. The mixing of sediment that occurs during lake formation can mask the existence of previous relatively shallow lakes. There is considerable uncertainty in the number of lakes of various sizes that might have existed in the Bonneville Basin. However, the main focus of the modeling is to ensure the presence of lakes that inundate Clive at different times in future glacial cycles, and to approximately match the net sedimentation of the past glacial cycles.

## 3.3 Shallow Lake Cycles

Smaller lake events have also occurred in the history of the Bonneville Basin. These are documented in Table 3 (C.G. Oviatt, Professor of Geology, Kansas State University, personal communication December 2010, January 2011, and email communication herein referred to as 'C.G. Oviatt, personal communication'). These events are evident when analyzing a pit wall interpretation at the Clive site (Appendix A; C.G. Oviatt, unpublished data) as well as at the ostracode and snail record present in the Knolls sediment core (Appendix B; C.G. Oviatt, unpublished data). The pit wall study conducted by Oviatt occured during early development of the Clive disposal facility. From the Clive pit wall interpretation, it is presumed that at least three shallow lake cycles occurred prior to the Bonneville cycle, although there is some uncertainty associated with that estimate. These shallow cycles could in fact be part of the transgressive phase (i.e., rising lake level) of the Bonneville cycle (C.G. Oviatt, personal communication). By analyzing the Knolls core interpretation, which is more representative of Clive than the Burmester core due to its relative proximity and differences in their regional topography, the Little Valley cycle is present at approximately 16.8 m from the top of the core. Given the pit wall at Clive was 6.1 m deep and does not capture the Little Valley cycle, it can be speculated that other smaller lake cycles occurred in the Clive region in addition to the three shallow lake events noted in Table 3 (labeled as Pre-Bonneville Lacustrine Cycles).

Of interest is that the deep lake cycle of Lake Bonneville did not result in substantial sediment deposition. Each shallower lake cycle, given that they probably occurred for shorter periods of time than Lake Bonneville, deposited sediments at a greater rate. Sediment can also accumulate during inter-glacial periods from air deposition, which is reworked when a lake returns. The Knolls core suggests that 16.8 m of sediment was deposited in the last glacial cycle. This also matches the Burmester core sediment record.

For modeling purposes, a distinction is made between shallow, intermediate and large lakes. Large lakes are assumed to be similar to Lake Bonneville, occurring no more than once per 100 ky glacial cycle. Intermediate lakes are assumed to be smaller lakes that reach and exceed the altitude of Clive, but are not large enough that carbonate sedimentation can occur. Shallow lakes are assumed to exist at all other times. The current Great Salt Lake is an example. Under current climate conditions, it is assumed that intermediate lakes will not occur. Under future climate conditions, some glacial cycles will produce a large lake in the Bonneville Basin, and intermediate lakes will occur during the transgressive and regressive phases of a large lake, or during glacial cycles that do not exhibit a large lake.

**Table 3. Lake cycles and sediment thickness from Clive pit wall interpretation (C. G. Oviatt, personal communication)**

| Lake Cycle | Thickness of Sediment Layer (meters) | Depth Below Ground Surface (meters) |
|---|---|---|
| Gilbert Lake transgressive/regressive phase | 1.05 | 1.05 |
| Lake Bonneville Regressive Phase (reworked marl) | 0.43 | 1.48 |
| Lake Bonneville Open Water (white marl) | 1.29 | 2.77 |
| Lake Bonneville Transgressive (littoral facies) | 0.76 | 3.53 |
| Pre-Bonneville Lacustrine Cycle 3 (possible shallow lake) | 0.71 | 4.24 |
| Pre-Bonneville Lacustrine Cycle 2 (possible shallow lake) | 0.62 | 4.86 |
| Pre-Bonneville Lacustrine Cycle 1 (possible shallow lake) | 1.14 | 6.00 |

## 3.4 Sedimentation

The types of sediment resulting from the formation and long-term presence of lakes in the Bonneville Basin can be divided into two components: 1) biogenic (i.e., sediment from biological processes), and 2) terrigenous (i.e., sediment that is mechanically and chemically eroded and transported). During the large pluvial lake events, biogenic sediment in the form of calcium carbonate was precipitated as tufas, marls, shells (of mollusks), and ostracodes (Hart et al., 2004). Terrigenous sedimentation however, accounts for the majority of sediment deposited throughout the sediment core record (C.G. Oviatt, personal communication). The geomorphological evidence in the form of various lake shorelines carved into the landscape in the Bonneville Basin is an example of the terrigenous erosional capacity of a deep lake system over long time periods. Given the difficulty in separating biogenic versus terrigenous causes of sedimentation, estimates reported below are assumed to be representative of cumulative sedimentation from all causes during a lake event. During inter-glacial periods air deposition also adds to the sedimentation, although there are no sediment core records of airborne sedimentation perhaps because the formation of each lake results in mixing of the upper range of existing sediments.

Brimhall and Merritt (1981) reviewed previous studies that analyzed sediment cores of Utah Lake, a freshwater remnant of Lake Bonneville that formed at approximately 10 ky BP. They suggest that up to 8.5 m of sediment has accumulated since the genesis of Utah Lake, implying an average sedimentation rate of 850 mm/ky over 10 ky. Within the Bonneville Basin as a whole the major lake cycles resulted in substantial accumulations of sediment based on the depth of the cores analyzed (e.g., a 110-meter core that corresponds to the past 780 ky, or four large lake cycles [Oviatt et al., 1999]), which averages about 140 mm/ky. Einsele and Hinderer (1997) indicate that sediment accumulation in the Bonneville Basin occurred at a rate of 120 mm/ky during the past 800 ky. The Knolls core suggests that there has been 16.8 m sedimentation in the last glacial cycle, or nearly 170 mm/ky.

Interpretations of the Clive pit wall (Table 3; C.G. Oviatt, unpublished data) indicate that the sedimentation rate at the Clive site for the Lake Bonneville cycle is on the order of 2.75 m over a 17-19 ky time period (140-160 mm/kyr). By contrast, shallow lacustrine cycles that occurred prior to Lake Bonneville (but after the Little Valley cycle) indicate that the amount of sediment deposited during each cycle is approximately 1/3 that of the Bonneville sediment deposited. The timing of these shallow lake cycles is uncertain, however it can be approximated when comparing the Clive pit wall interpretation to the Knolls Core (C.G. Oviatt, personal communication). The Little Valley lake cycle is exhibited in the Knolls Core at a depth of approximately 17 m, which is roughly 14 m deeper than the beginning of the transgressive phase of the Bonneville lake cycle event noted on the Clive pit wall interpretation. Given the Little Valley event occurred 150 ky BP, a sedimentation rate can be approximated for the depth between this event and the transgressive phase of the Bonneville cycle of 110 mm/ky.

These data support greater sedimentation rates in shallow lakes (sedimentation in Utah Lake is much greater, and sedimentation in the Clive Pit Wall indicates lower rates for a deep lake cycle), but also suggest that the sedimentation rate in each glacial cycle is similar.

# 4.0 Conceptual Overview of Modeling Future Lake Cycles

As stated in the overall Conceptual Site Model (Neptune, 2011a), there is a lack of peer-reviewed literature that allows accurate and precise prediction of the direct effects of future climate change on major lake formation in the Bonneville Basin. However, assuming no major changes from recent climate cycles, the probability of another major lake cycle occurring in the Bonneville basin within the next few million years is high. Variations in the Earth's orbital parameters in combination with increases in inputs of freshwater into the world's oceans are likely to lead to another major ice age and could alter long-term climatic patterns in the Bonneville Basin, resulting in deep lake formation. It is possible that the Clive facility will be subjected to deep lake formation in the future, unless anthropogenic effects on atmospheric $CO_2$ concentrations cause major changes in climatic patterns (Berger and Loutre, 2002).

The basic intent of the deep-time model is to allow lakes to recur in the Bonneville Basin that are sufficiently large that the above-ground portions of the DU waste embankment will be obliterated, and so that the sedimentation rates for each glacial cycle are similar. The exact timing of the recurring lakes is not important, the current 100 ky cycle excepted. The deep-time model allows a deep lake to return in each 100 ky cycle, which, given the scientific record, might be conservative. It also allows intermediate lakes to recur at a frequency that allows the 100 ky sedimentation rate to be satisfied. The current 100 ky cycle is not modeled explicitly. It is possible that the current inter-glacial period will last for another 50 ky, which is unusually large.

The return of a large lake causes the above-ground features of the site to be obliterated, and the contents of the waste embankment to be dispersed through wave action. The DU waste is assumed to be mixed with lake sediments. Each new lake event causes more sedimentation, which will either bury or continually mix the waste with more sediment over time. This basic conceptual model is described in more detail below.

**Future Scenarios**

Various Features, Events, and Processes (FEPs) may be associated with the effect of a lake return scenario on the DU waste embankment, including wave action, sedimentation, and site inundation. Details of the FEPs process are provided in the *Features, Events and Processes for the Clive DU Performance Assessment* report (Neptune, 2011b). Starting with current conditions, representative lake occurrence scenarios for the long-term future are described below and depicted in Figure 3. Note that there are two components of the models used to represent these scenarios. The first is modeling lake formation and dynamics, based upon the scientific record. The second is modeling the fate of the DU waste embankment.

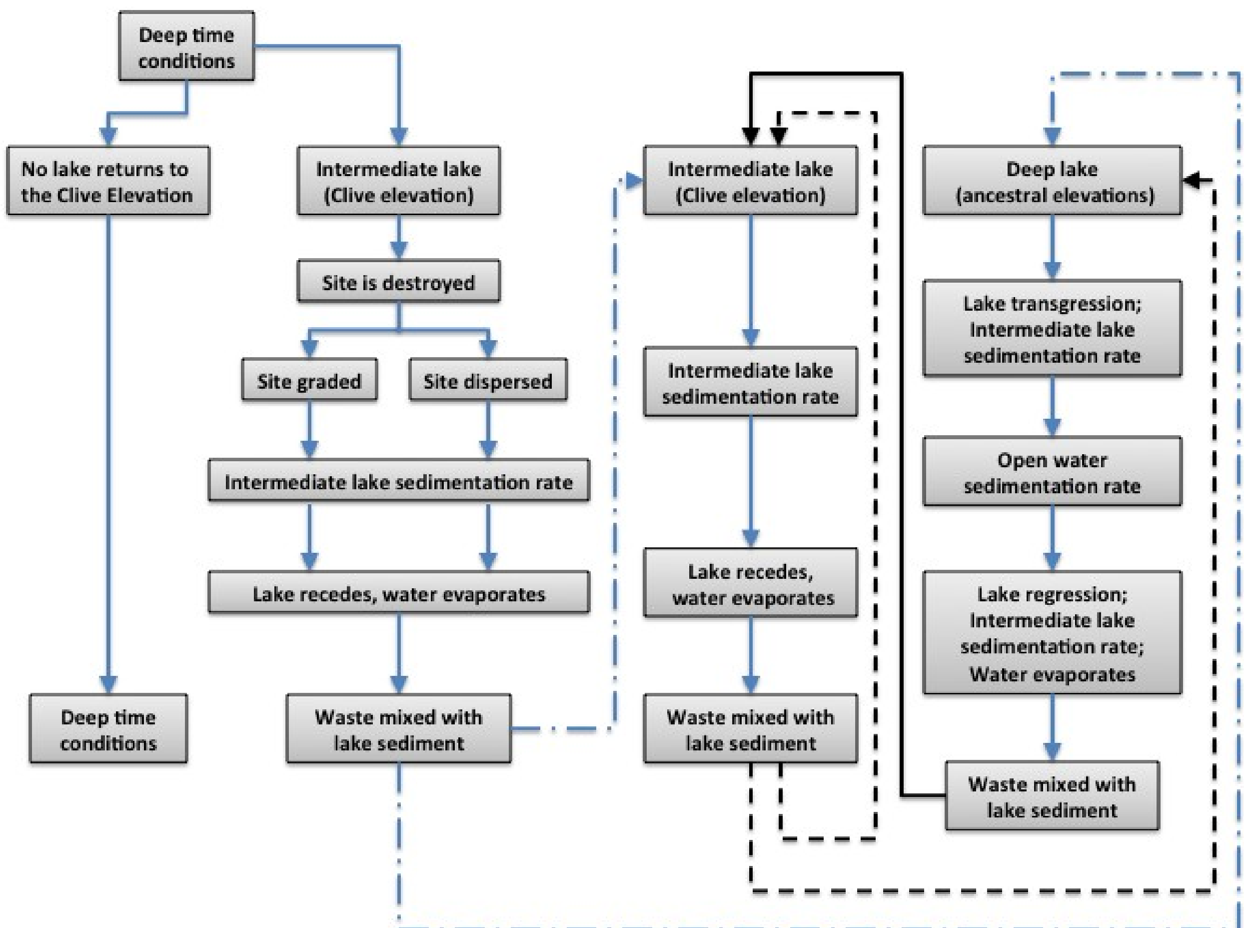


**Figure 3. Scenarios for the long-term fate of the Clive facility**[5]

5 The scenario that indicates that no lake returns to the Clive elevation implies that a shallow lake is present and never reaches the Clive site.

The Great Salt Lake represents the current condition of a lake in the Bonneville Basin. Lakes such as this are likely to exist in all future climatic cycles, but lakes that do not reach the elevation of the DU waste embankment at Clive will not affect the waste embankment. For the Clive DU waste PA model, it is assumed that destruction of the waste embankment will result from the effects of wave action from an intermediate or large lake. In effect, it is assumed that a lake is large enough that obliteration of a relatively soft pile will occur. This assumption separates shallow and intermediate lakes. In this obliteration scenario, all of the embankment material above grade is assumed to be dispersed through a combination of physical dispersal through wave action and dissolution into the water column above the waste dispersal area.

Waste material that dissolves into the lake eventually returns to the lake bed through precipitation or evaporation as the lake regresses.

While the lake is present, some waste in the water column will bind with carbonate ions and precipitate out into ooilitic sediments, while the remaining waste will fall out with the sediment as the lake eventually recedes. The waste material enters the lake system, creating lake water concentrations. However, all of the waste re-enters the lake sediment once the lake disappears. Sediment concentrations decrease over time because the amount of waste does not change other than through decay and ingrowth, whereas more sediment is added over time.

The model assumes the waste is fully mixed with the accumulated sediment, whereas some waste might be buried by future lake sediments. The model also allows large dispersal areas, and assumes a water column for accepting waste through dissolution that is contained above the dispersal area. These assumptions are conservative, leading to greater concentrations of waste than is probably reasonable. The conservatism is included in this model because of the lack of data that exists to quantify the processes. For example, the extent of mixing of previous sediment with new sediment is not understood, hence an assumption that the sediments completely mix is expedient, but is conservative, since it retains some of the waste near the surface rather than burying it under the latest cycle of sedimentation. Limiting dissolution to a column above the waste dispersal area is conservative because lake water will probably mix more extensively, but the dispersal area is difficult to estimate. An approach that considers the size of the spits from from the Grayback Hills to the north of the Clive facility that were formed during the lake event might provide a better analog. It should be noted that a Gilbert-sized lake would just barely reach Clive and the wave energy would very likely not erode the waste embankment (C. G. Oviatt, personal communication). The size of lake in the PA model that is needed to obliterate the waste embankment can be as small as 1 m, which might not have sufficient wave power to obliterate the site. Dissolution into such a shallow lake might over-estimate lake water concentrations, if such a shallow lake cannot obliterate the waste embankment. There are various reasons why the deep time model might over-estimate lake water and sediment concentrations, but the data needed to better specify the model are not readily available. Depending on the model performance, data collection in support of model refinement might prove to be desirable.

One other factor that is important for this model is that the lake formation model is applied to each 100 ky cycle similarly. That is, the current 100 ky cycle is not treated differently, despite evidence that the current inter-glacial period might last for another 50 ky (Berger and Loutre, 2002). In the model, therefore, an intermediate lake can return sooner than might be expected in the current 100 ky cycle. From the perspective of obliteration of the embankment, the timing is largely irrelevant. The mass of waste does not change much over time. However, the deep-time model also assumes that the form of DU available for deep-time transport is $U_3O_8$, which is far less soluble than $UO_3$ (see *Radioactive Waste Inventory for the Clive PA* (Neptune, 2011c)). The DU waste consists primarily of $U_3O_8$, from the gaseous diffusion plants. However, the form of the DU waste from the Savannah River Site is $UO_3$. Fate and transport modeling performed in the GoldSim PA model indicates that the $UO_3$ will have completely or almost completely migrated to groundwater within 50 ky. Consequently, the deep time model focuses on $U_3O_8$ as the form of DU available for deep-time migration.

The remainder of this section describes the specifics of the models that have been developed for this PA, including lake formation and sedimentation.

### 4.1.1 Intermediate and Large Lake Formation

This scenario assumes that changes in climate will continue to cycle in a similar fashion to the climate cycles that have occurred since the onset of the Pleistocene epoch. These changes follow those observed in the marine oxygen isotope record (Figure 2). The record captures major climate regime shifts on a global scale and are used in this scenario in conjunction with expert opinion (C.G. Oviatt, personal communication) and site-specific sediment core and pit wall information to determine the approximate periodicity of lake events. However, uncertainties exist due to the limitations related to the quality of the sediment core data. The following subsections provide more detail with respect to the assumptions for both intermediate and large lake formation.

#### 4.1.1.1 Intermediate Lake Formation

The Great Salt Lake represents the current condition of a lake in the Bonneville Basin. Lakes such as this are likely to exist for periods of time during all future climatic cycles, but lakes that do not reach the elevation of the DU waste embankment at Clive will not affect the waste embankment, so they need are not modeled explicitly. However, it is assumed that during the 100 ky climatic cycles, larger lakes will occur, including lakes that reach the elevation of the DU waste embankment at Clive. Although a definitive distinction is not made, lakes that reach the elevation of Clive but do not develop into a large lake are considered intermediate lakes. These intermediate lakes are also assumed to be large enough that their wave action will destroy the waste embankment. Intermediate lakes might occur during the transgression and regression phases of a large lake, or might occur during a glacial cycle that does not produce a large lake, perhaps in conjunction with glacial cycles that are shorter and less severe than the 100 ky year glacial cycles previously discussed (for example, potentially the current 100 ky cycle).

In general, variation in lake elevation is assumed to occur at all lake elevations. The variation is due to local temporal changes in temperature, evaporation and precipitation. For example, the Great Salt Lake has seen elevation changes of several tens of feet in the past 30-40 years. In addition, the Great Salt Lake has seen greater elevation changes in the past 10 ky, but in no cases since the Younger Dryas has the Great Salt Lake reached the elevation of Clive.

Sedimentation is assumed to occur during these intermediate lake events at greater annual rates than is assumed to occur for the open-water phase of large lakes. This is based on the pre-Bonneville lacustrine cycles that are documented in Table 3 (Clive pit wall interpretation – see Appendix A). The lake is assumed to recede after some period of time, at which point a shallow lake relative to the Clive facility will occupy Bonneville Basin until the next intermediate or large lake cycle. The details relating to the mathematical approach employed to model this scenario and model parameters are provided in Section 6.0.

#### 4.1.1.2 Large Lake Formation

In this scenario, a large lake forms throughout the Bonneville Basin in response to major glaciation in North America and the Northern Hemisphere, following the ongoing 100 ky glacial cycle. Increases in precipitation and decreases in evaporation over the long-term, and subsequent increases in discharge to the Bonneville Basin via rivers that drain high mountains along the eastern side of the basin in general have resulted in lakes that are more than 30 m deep and cover an area similar to that of the most recent pluvial lake episode (e.g., Lake Bonneville, Provo Shoreline). This same extent of lake formation is assumed to occur in the future. Under such a scenario, the depth of a lake at the location of the Clive facility could be many tens of meters, resulting in sedimentation over the long period of time of the lake's existence. A key difference between this scenario and the intermediate lake scenario is that both the transgressive and regressive phases of lake formation are considered. Transgressive and regressive phases of lake formation can lead to brief periods of rising and falling water levels in both phases. These phases of transgression and regression are also assumed to have higher sedimentation rates than the open-water phase. Upon the complete regression of a large lake, it is assumed that only intermediate lakes will form until the large lake associated with next 100 ky climate cycle occurs. It is assumed that destruction of the waste embankment occurs in response to the formation of a large lake, if the first large lake occurs prior to formation of an intermediate lake.

## 5.0 A Heuristic Model for Relating Large Lakes to Climate Cycles from Ice Core Temperature

In this section, a model is presented for estimating lake elevation that uses surface temperature deviations from the EPICA Dome C ice core data (Jouzel et al., 2007). The model is not intended to be highly accurate, but rather is aimed at capturing the major lake-cycle features as shown in the studies conducted by Oviatt et al. (1999), Link et al. (1999), and the sediment core and pit wall interpretations (C.G. Oviatt, personal communication). This model is not used as a predictive model but rather to form a basis for the character and dynamics of lake events, which will be implemented in the deep time model developed in Section 6.0.

The deep-sea benthic $\delta^{18}O$ record is in excellent agreement with the EPICA Dome C deuterium measurements for the last approximate 810 ky (Jouzel et al., 2007). Temperature anomaly data for the past 810 ky were obtained from the World Data Center for Paleoclimatology, National Oceanic and Atmospheric Administration/National Climate Data Center. These data are made available based on calculations described in Jouzel et al. (2007), and are plotted in Figure 4. From the 810 ky of data, the temperature deviations range from $T_{min} = -10^{o}C$ to $T_{max} = +5^{o}C$. This range is utilized to bound extreme events.

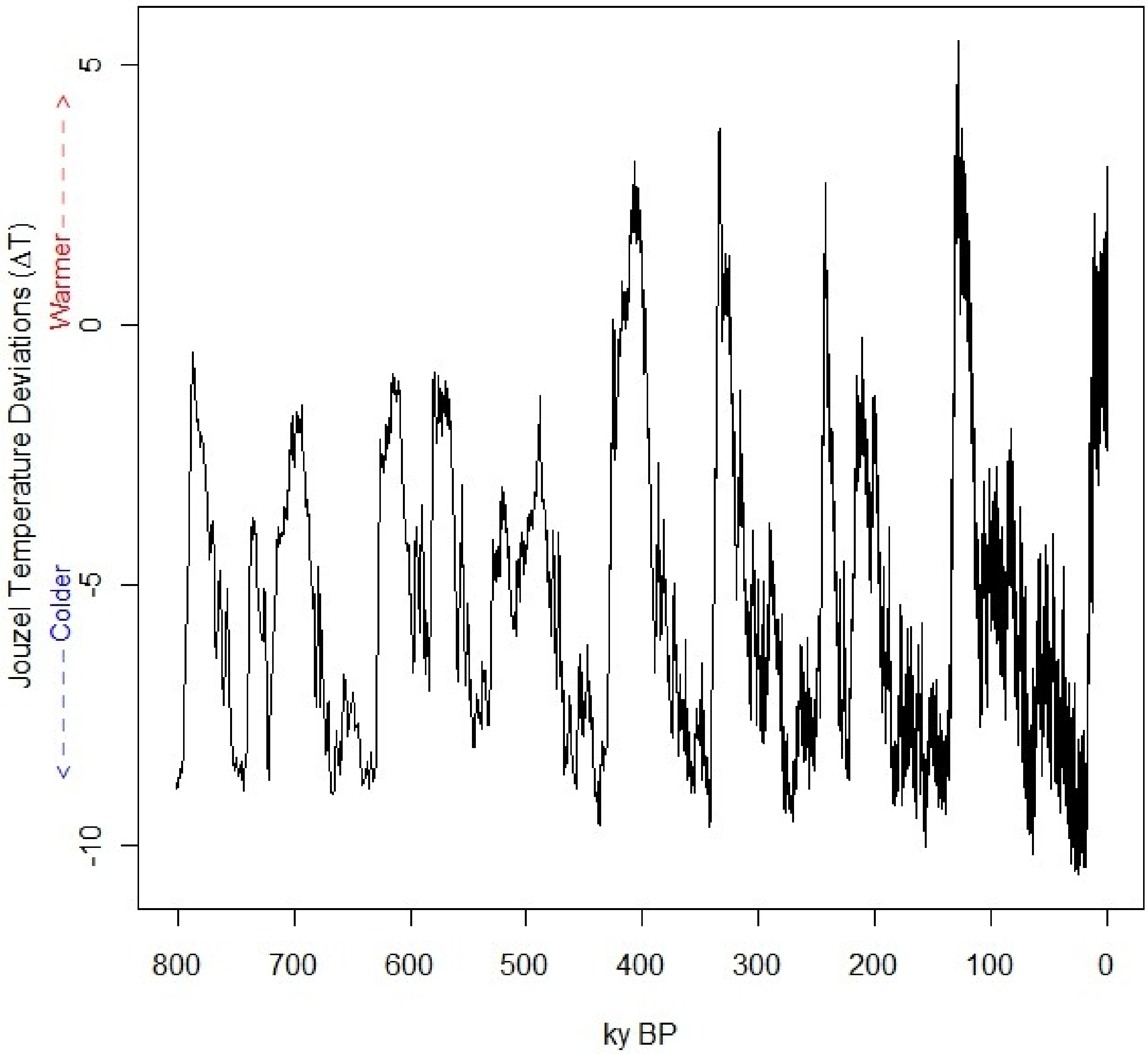


**Figure 4. Temperature deviations for the last 810 ky, Jouzel (2007).**

## 5.1 Conceptual Model

Water balance in the Bonneville Basin is affected by many complex processes, so modeling water balance simply as a function of temperature alone is not expected to produce any precise results, but might succeed in representing a coarse feature. The conceptual model is based on a water balance reservoir model of precipitation versus evaporation. If precipitation outpaces evaporation, the lake elevation increases. If evaporation outpaces precipitation, then the lake elevation decreases. Precipitation and evaporation are affected directly by temperature, but long term patterns of precipitation are affected more greatly by the presence or absence of continental glaciation in North America. Thus, glaciation is modeled first using a simple reservoir model depending on temperature.

## 5.2 Glaciation

The water balance model begins by constructing a "continental glacier" – an artificial construct that represents a glacier large enough to affect precipitation levels in the Bonneville Basin. The extent of glaciation in proximity to the Bonneville Basin is assumed to be zero initially, which is a reasonable approximation for the start time of 785 ky BP, a start time chosen because it corresponds to a warmer climate phase (data from Jouzel, et al., 2007 – see Figure 4). For each time step of 500 years, an increase in glacial magnitude is dependent on temperature deviation ($\Delta T$) as scaled in Jouzel (see Figure 4):

$$Glacial_{addition}(\Delta T) = \begin{cases} 0 & \text{if } \Delta T \geq \Delta T_{GMax} \\ \frac{1}{N_{GA}}\left(e^{R_{GA}\cdot(\Delta T_{GMax} - \Delta T)} - 1\right) & \text{if } \Delta T < \Delta T_{GMax} \end{cases} \tag{1}$$

where

- $N_{GA}$ is a normalizing constant:

$$N_{GA} = e^{R_{GA}\cdot(\Delta T_{GMax} - \Delta T_{min})} \tag{2}$$

- $R_{GA}$ is a rate parameter ($yr^{-1}$), and
- $T_{GMax}$ is a threshold temperature (degrees Celsius).

Since the glacier is an artificial construct for modeling purposes, the units and scale of the glacial "magnitude" are arbitrary. The parameters of the precipitation model described below must be calibrated appropriately to the scale of the glaciation model.

For each time step, the decrease in glacial magnitude is also modeled as a function of temperature:

$$Glacial_{subtraction}(\Delta T) = \begin{cases} 0 & \text{if } \Delta T \leq \Delta T_{GMin} \\ \frac{S_{GS}}{N_{GS}}\left(e^{R_{GS}\cdot(\Delta T - \Delta T_{GMin})} - 1\right) & \text{if } \Delta T > \Delta T_{GMin} \end{cases} \tag{3}$$

where

- $N_{GS}$ is a normalizing constant:

$$N_{GS} = e^{R_{GS}\cdot(\Delta T_{max} - \Delta T_{GMax})} \tag{4}$$

- $R_{GS}$ is a rate parameter ($yr^{-1}$), and
- $T_{GMin}$ is a threshold temperature (degrees Celsius).

The change in glacial magnitude for a time step is thus:

$$Glacier_t = max\left\{0, Glacier_{t-1} + Glacial_{addition}\left(\Delta T_t\right) - Glacial_{subtraction}\left(\Delta T_t\right)\right\} \tag{5}$$

where the $t$ subscript is a time step index. The time step used for the model is 500 years.

The parameters of the model were calibrated heuristically to compute parameters that produced a glacial cycle that appeared reasonable for this coarse model. The set of parameters computed was:

$$\Delta T_{GMax}=-6\,;\,R_{GA}=0.25\,;\,\Delta T_{GMin}=-6\,;\,R_{GS}=0.2\,;\,S_{GS}=5 \tag{6}$$

The change in the glacial magnitude for a particular time step as a function of temperature is shown in Figure 5. These values lead to slow growth during the very cold phases (Jouzel temperature deviations of less than -6 °C) of the glacial cycle, and rapid recession during warm phases (Jouzel temperature deviations of greater than -6 °C).

## 5.3 Precipitation

A coarse model for precipitation in the Bonneville Basin was developed dependent on global temperature (as precipitation generally increases with global temperature), lake surface area (which affects recharged evaporation), and an additional effect that depends of the magnitude of the continental glacier. The precipitation in meters of annual rainfall is modeled as:

$$P_t\left(\Delta T_t, L_{t-1}, G_{t-1}\right)=B_P+R_{PT}\cdot\Delta T+R_{PLSA}\cdot SA\left(L_{t-1}\right)+S_{PG}\cdot e^{R_{PG}\cdot G_{t-1}} \tag{7}$$

where $B_P$ is a baseline precipitation, $R_{PT}$ is a coefficient of linear effect of global temperature, $R_{PLSA}$ is a coefficient of linear effect of the surface area of the lake, and $SA(L)$ is the surface area in $km^2$ associated with lake elevation $L$. The effect of temperature and lake surface area are modeled as linear, while the glacial effect is exponential with respect to glacier size. The set of parameters calibrated to the glacial magnitude model are:

$$B_P=0.30\,;\,R_{PT}=0.005\,;\,R_{PLSA}=2\text{e-}6\,;\,S_{PG}=0.06\,;\,R_{PG}=0.03 \tag{8}$$

The precipitation is then converted to a volume by multiplying by the area of Bonneville Basin (approximately 47,500 $km^2$).

## 5.4 Evaporation

Evaporation rate in the region is modeled as a function of temperature:

$$E_t\left(\Delta T_t\right)=B_E+\frac{S_E}{N_E}\cdot e^{R_E\cdot\left(\Delta T-\Delta T_{min}\right)} \tag{9}$$

where $N_E$ is a normalizing constant:

$$N_E=e^{R_E\cdot\left(\Delta T_{max}-\Delta T_{min}\right)} \tag{10}$$

The evaporation is then converted to a volume by multiplying by the area of the basin.

The calibrated parameters are:

$$B_E=0.32\,;\,S_E=0.3\,;\,R_E=0.05\,;\,\Delta T_{min}=-10\,;\,\Delta T_{max}=5 \tag{11}$$

If the precipitation volume exceeds the evaporation volume, then the difference is added to the lake volume, and the lake elevation is calculated from the total lake volume.

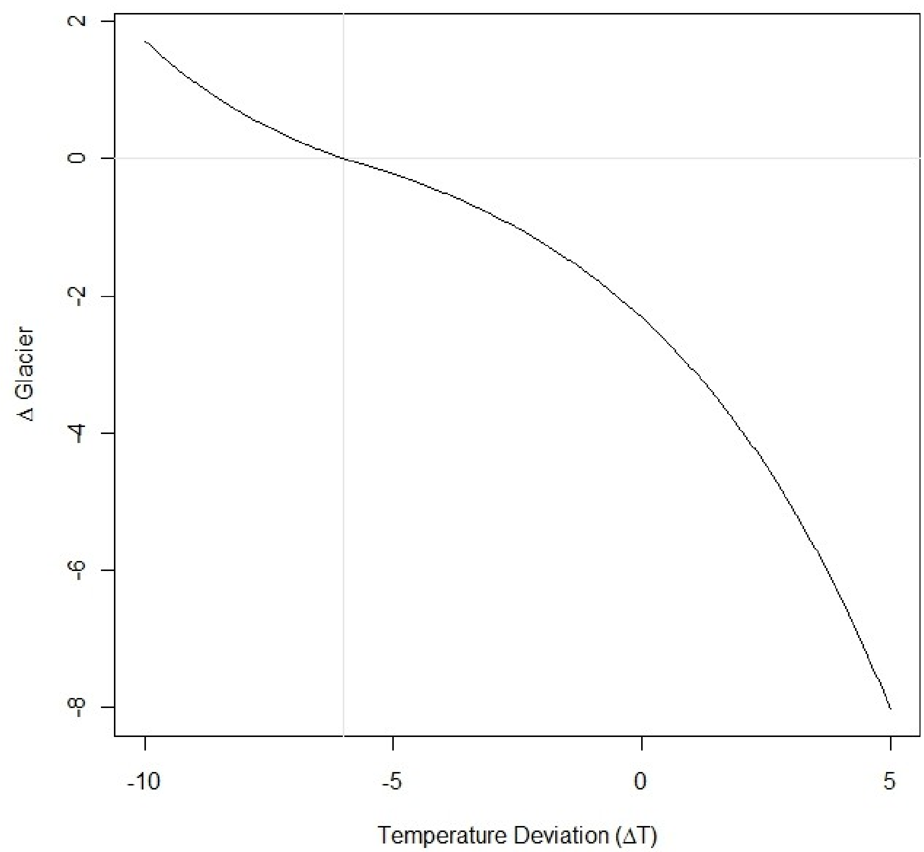


**Figure 5. Glacial change as a function of temperature for the coarse conceptual model.**

If the evaporation volume is greater than the precipitation volume, then the total evaporation is adjusted downward to adjust for the actual surface area exposed (rather than the full surface area of the basin as used in the initial calculation). The difference between the adjusted evaporation and the precipitation is then subtracted from the lake volume, and the lake surface elevation is calculated from the total lake volume.

$$\Delta\, Volume_t = \begin{cases} \left[P_t(\Delta T_t) - E_t(\Delta T_t)\right] \cdot SA_{basin} & if\ E_t(\Delta T_t) < P_t(\Delta T_t) \\ \left[P_t(\Delta T_t) - E_t(\Delta T_t)\right] \cdot \dfrac{SA(L_{t-1})}{SA_{basin}} & if\ E_t(\Delta T_t) \geq P_t(\Delta T_t) \end{cases} \quad (12)$$

## 5.5 Simulations

For simplicity, the lake volume and glacial magnitude are assumed to be zero at the first time step (785 ky BP), as that time step corresponds to a warm climate phase. The values for the parameters given above are calibrated graphically to produce reasonable precipitation versus evaporation values. Several lake elevation histories were simulated by simulating the parameter values of the model probabilistically. The distributions for the parameters were lognormal with medians equal to the parameter values listed in Equations (6), (8), and (11). The simulations provide a variety of behaviors depending on the combination of parameters simulated.

A few common features are apparent in the simulated results. The largest lakes tend to occur at the times of Lake Bonneville, Little Valley, and Lava Creek, and the smallest 100 ky cycle lake occurs in $\delta O^{18}$ cycle 14 (~533 ky BP), which matches the scientific record. When the simulated glaciation effects are small ($R_{GA}$ and $R_{GS}$) , precipitation change in the model is due primarily to temperature change. In this case, large lakes form with few intermediate lakes, as the lake elevation history in the top graph in Figure 6 shows. When glaciation effects are larger, then large lakes tend to last longer, and intermediate lakes form, as the lake elevation history in the lower graph of Figure 6 shows.

The simulation models were then calibrated further by combining the simulated lake histories with sedimentation rates seen in sediment cores. Based on the results of this coarse model calibration, some assumptions are carried forward to the deep time model.

1. The 100 ky cycle in global temperature is a strong indicator of the return of a large lake. While not all simulations showed a lake returning to the Clive elevation in every 100 ky cycle (particularly $\delta O^{18}$ cycle 14), the results were consistent enough to treat as systematic behavior for a heuristic model.
2. Intermediate lakes should be a part of the deep time simulation, because sedimentation rates did not calibrate well with simulations that produce only large lakes.
3. Intermediate lakes are more likely to occur in the later stages of the 100 ky cycle than in the early stages, primarily in conjunction with the slowly decreasing temperatures across the cycle (as opposed to the relatively rapid warming period that occurs at the end of a 100 ky cycle).

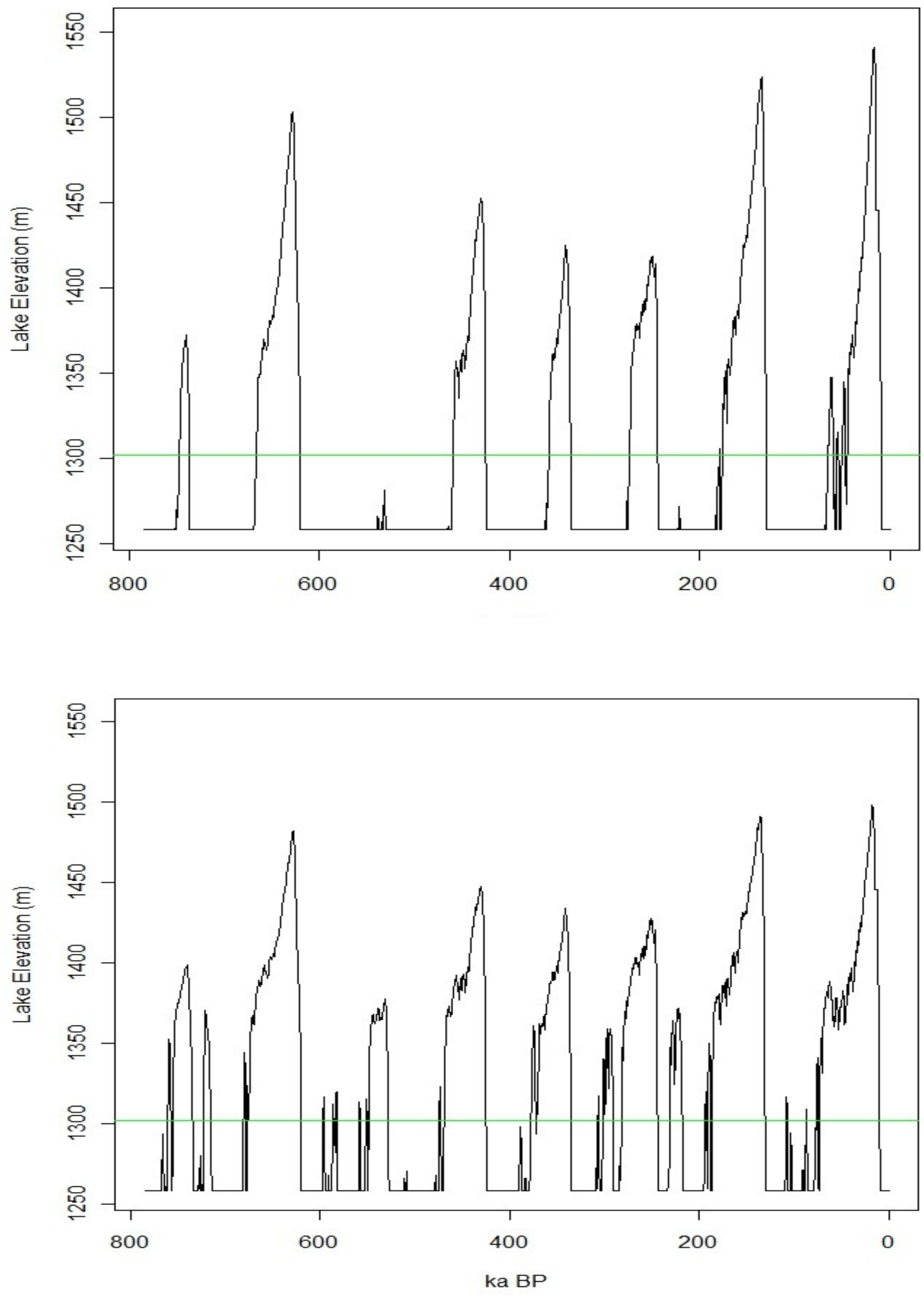


**Figure 6. Two example simulated lake elevations as a function of time with Clive facility elevation represented by green line.**

# 6.0 Modeling Approach for the PA Model

Depleted uranium, since it is primarily $^{238}U$, has the property of becoming more radioactive with time, due to the ingrowth of decay products that were separated out during processing. The extremely long half-life of $^{238}U$ regulates this ingrowth, and the DU waste gets more radioactive over a period of about 2.1 My, and remains at that constant activity for billions more years. It is therefore of interest to understand, at least at a qualitative level, what the distant future (beyond 10,000 y) holds for the Clive facility. This deep time modeling includes what might be expected over those 2.1 My, in a stylized depiction of the effects of lakes returning to the Bonneville Basin.

With the return of the first lake that inundates the site, contaminant transport modeling within embankment ceases, and those above-ground portions of the facility are assumed to be obliterated and dispersed to varying degrees. While the lake is present, the dispersal of the site is coincident with dissolution of wastes into the water column, and their burial under fresh lacustrine sediments. Modeling the details of such processes is beyond the scope of this PA, but gross estimates of radionuclide concentrations in sediments and in the lake water are made. The long term concentrations of long-lived isotopes and their decay products are of primary concern. A detailed, precise model of temporal lake cycles is therefore not necessary—rather, a model that captures the major features of lake recurrence is indicated. The basic features of the heuristic lake formation model presented in Section 5.0 are abstracted into the Clive DU PA Model to construct a probabilistic model for the deep time model. The various components of this model are presented here.

## 6.1 Large Lakes

The 100 ky climate cycle is treated as a sufficiently robust effect to create a hypothetical lake that will reach the elevation of Clive each cycle. The exact time of occurrence is not a crucial parameter, due to the slowly-changing concentrations during deep time. Thus, the lake is set to be present at each 100 ky mark, with time beginning at 10 ky (the end of the quantitative performance period addressed for the quantitative dose assessment component of the PA).

There is little information on the amount of time that the Clive location has been under water. Lake Bonneville has been estimated to have been present at the elevation of Clive for a duration of approximately 16,000 years (Oviatt et al., 1999). Durations of older large lakes are unknown. Thus, a conservative choice was made to allow large lakes to endure an average of about 20,000 years (conservative in the sense that more waste will migrate into the water column). The occurrence time for each large lake is set by choosing a start time some number of years prior to the 100 ky mark. The start time is represented by a lognormal distribution with geometric mean of 14 ky prior to the 100 ky mark, and a geometric standard deviation of 1.2. The end time is represented by a lognormal distribution with geometric mean of 6 ky after the 100 ky mark, and a geometric standard deviation of 1.2. These distributions are depicted in Figure 7.

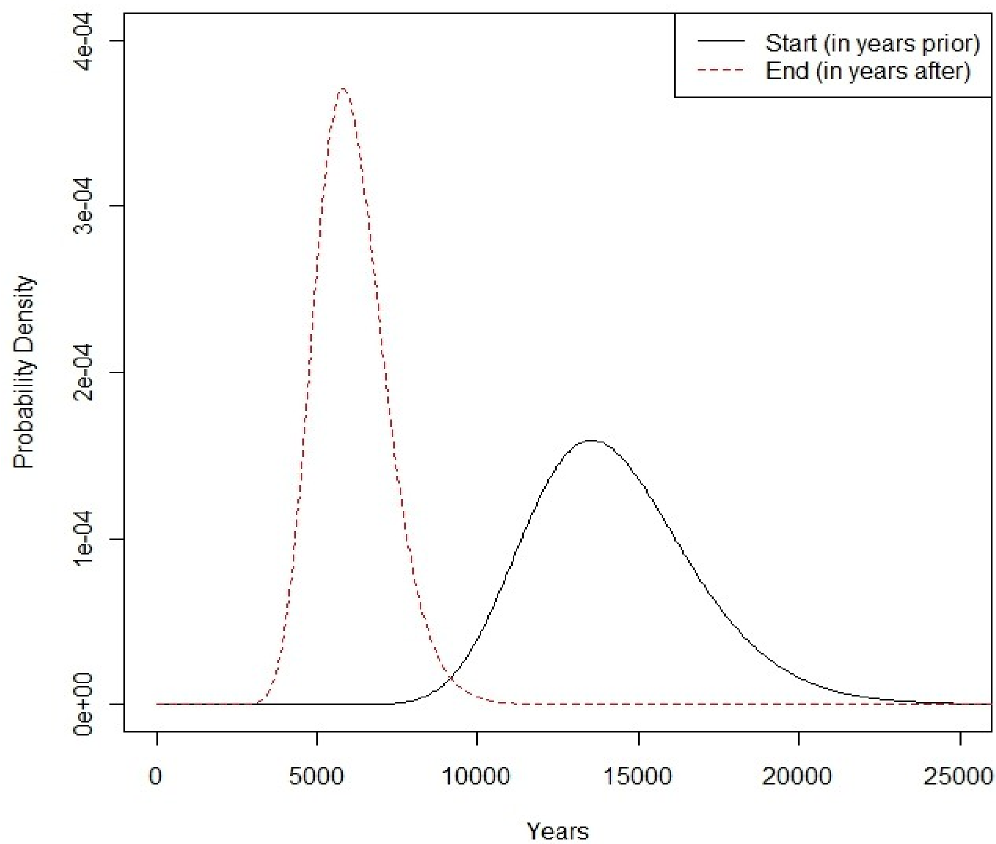


**Figure 7. Probability density functions for the start and end times for a large lake, in years prior to the 100 ky mark and years after the 100 ky mark, respectively.**

## 6.2 Intermediate Lakes

Intermediate lakes are modeled as potentially occurring anytime between large lake events. In order to reflect the slow decrease in temperature over the 100 ky cycle, the occurrence time for intermediate lakes is modeled as a Poisson process with a rate that increases linearly over the cycle time, from a rate of 0 to 7.5 lakes per 100 ky. This process produces an average of about 3 intermediate lakes per 100 ky. There is little recorded basis for this number, but it matches reasonably with the heuristic model of Section 5.0, and was chosen so that long-term sedimentation rates matched the average from previous lake cycles, as estimated from the sedimentation of individual lakes developed in Section 6.3.

There is virtually no information for the duration of intermediate lakes, due to the high mixing rate of shallow lake sediments, which makes dating of times within a single stratigraphic layer of a shallow lake sediment core extremely difficult. Thus, a distribution was chosen to roughly calibrate with the heuristic model: lognormal with geometric mean of 500 y and geometric standard deviation of 1.5.

## 6.3 Sedimentation Rates

Deposition of material in the area of the Clive facility is a continuous process that occurs during shallow, intermediate and large lake periods. During shallow lake periods, as observed in present-day conditions, air deposition is the primary mechanism. However, air deposition is not evident in sediment cores, presumably because of mixing with lake-derived sediments. Intermediate lake sediments include both terrigenous and oolitic content, with the ratio probably depending on the size and duration of the lake. Any airborne deposition is mixed with the sediments from the first returning lake. However, since air deposition layers are not evident in the sediment cores, the model effectively includes combines material from air deposition with material from lake sediments. The mixing probably occurs with an intermediate lake, which is likely to be the first lake after the inter-glacial period. This also suggests that there is a mixing depth associated with each lake recurrence. However, the mixing process itself makes it very difficult to associate mixing depth with the different layers in the sediment cores.

Large lakes, instead, have similar deposition rates to intermediate lakes in the transgressive and regressive phases, but a different, slower, rate when the lake is large enough that the dominant sedimentation is carbonate in nature. Records from the sediments cores are able to distinguish between layers associated with intermediate lakes that might include mixing of material from air deposition, terrigenous lake deposition, and oolitic lake deposition, and those associated with a stable large lake that are dominated instead by carbonate deposition.

Based on the available data from the sediment cores, sedimentation rates are expected to be higher when lake water is shallow than when a deep lake covers the Clive site.

For large lakes, a sedimentation rate is modeled as a lognormal distribution with geometric mean of 120 mm/ky and geometric standard deviation of 1.2, a distribution that covers the range of observed values for deep lakes in Section 3.4. This distribution is represented in Figure 8. The sedimentation rate is applied for the simulated duration of the large lake. In addition, sedimentation is added at the beginning of the lake cycle as well as the end that represents the shallow phase of the transgressive and regressive lakes. This additional sediment mimics the behavior of an intermediate lake.

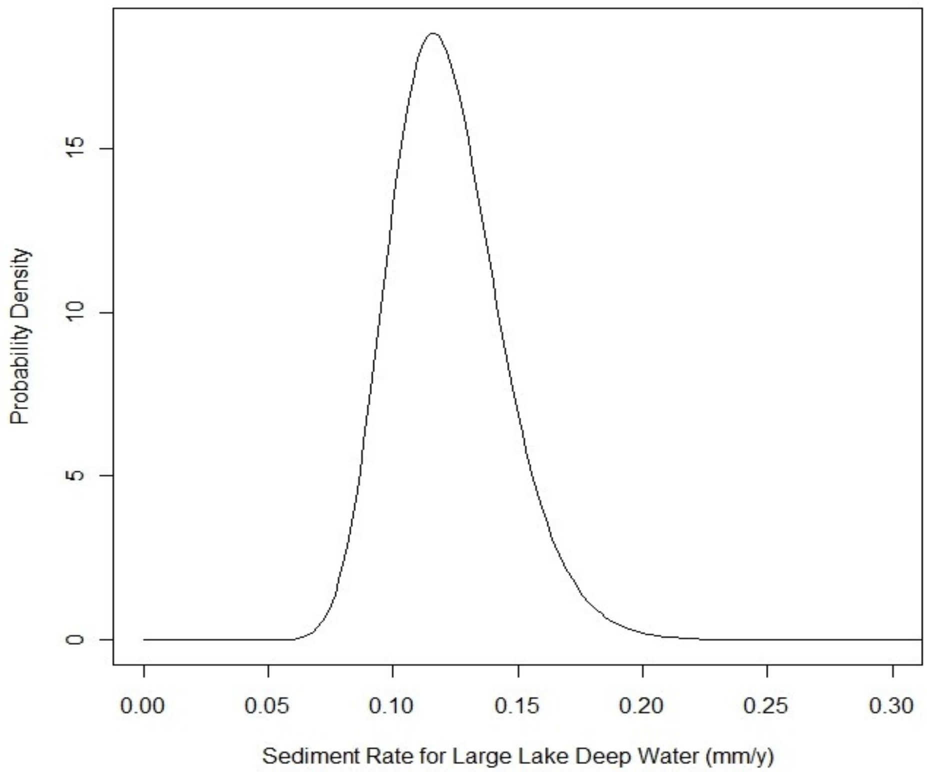


**Figure 8. Probability density function for sedimentation rate for the deep-water phase of a large lake.**

For intermediate lakes (and shallow phases of large lakes), there is high likelihood of multiple short-term transgressions and regressions with respect to the elevation of Clive. For example, the Clive pit wall (Appendix A) shows three distinct lakes after the deep-water phase of Lake Bonneville and three distinct lakes prior to the deep-water phase of Lake Bonneville. Without further study of a sediment core at the site, including dating, it is impossible to determine if these distinct lakes were separated by a few years or a few hundred years; i.e., whether they are distinct lake events or simply part of the transgression and regression of Lake Bonneville. However, based on current behavior of the lake, some year-to-year variation in the lake elevation occurs, in addition to the longer-term trends in lake elevation.

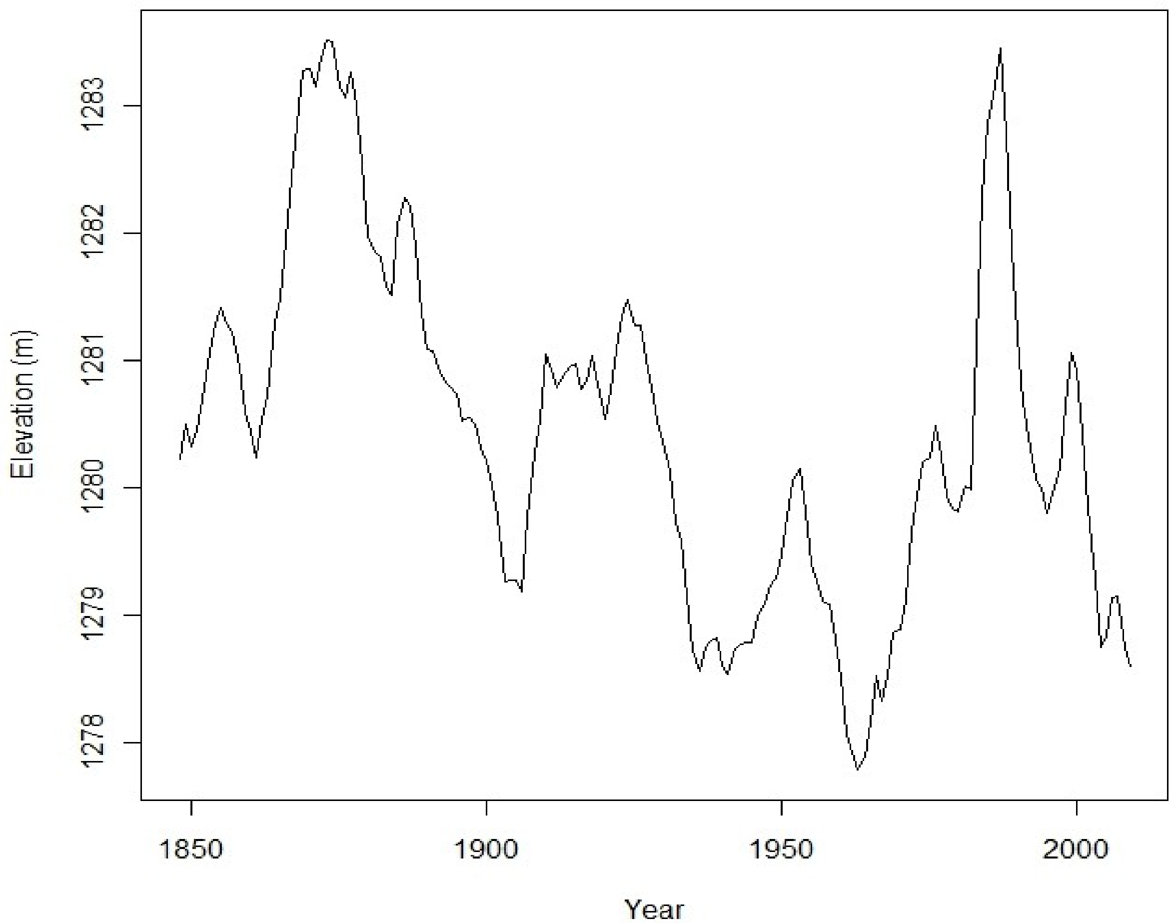


**Figure 9. Historical elevations of the Great Salt Lake.**

Another heuristic model was constructed to evaluate the effect of the short-term variation. The lake elevation for the years 1848 through 2009 is available from the Saltair Boat Harbor monitoring site (USGS, 2001), as shown in Figure 9. The year-to-year variation can be modeled as a second-order autoregressive process AR(2) (Brockwell and Davis, 1991), a model that accounts for year to year temporal correlations in the variation. An AR(2) process was simulated and added to a transgressive or regressive curve based on the simplified model of Section 5.0. Examples of these simulations are given in Figure 10. As can be seen in the figure, the short-term variation can result in lakes covering the Clive elevation for a short time, receding for a short time, then rising again, often multiple times in a single transgression. A similar simulation was performed for simulated intermediate duration lakes as well. The transgressive and regressive phases of a large lake behaved similarly to the intermediate lakes in that they averaged about 4 total occurrences of "mini-lakes;" i.e., occurrences of a rise above the elevation of Clive followed by a drop below for at least one year.

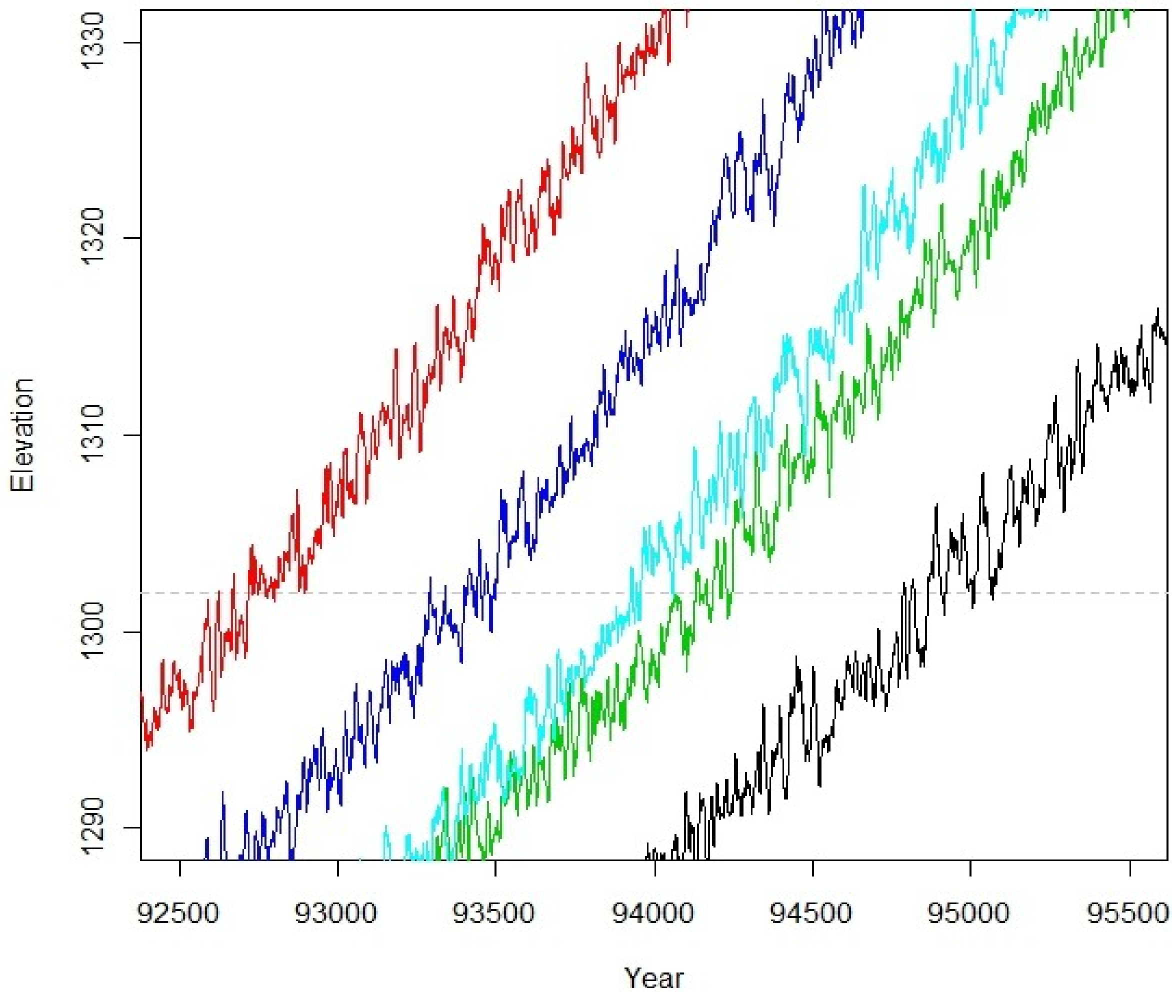


**Figure 10. Simulated transgressions of a large lake including short-term variation.**

The distribution for sedimentation rates for intermediate lakes was thus based on simulating this multiple mini-lake behavior. First, the number of mini-lakes associated with an intermediate lake was simulated as 1 plus a Poisson random variable with rate 3 (the "plus 1" being necessary to ensure at least one event in order to match the definition of a lake event). The sedimentation for each mini-lake was simulated according to a distribution based on the information for mini-lakes in the Clive pit wall, using the six distinct "mini-lakes" in Table 3 (all layers except the one that corresponds to the deep-water phase of Lake Bonneville), which resulted in a lognormal distribution with geometric mean 0.75 m and geometric standard deviation 1.4. The total sedimentation for all mini-lakes associated with a simulated intermediate lake cycle were then added together to produce a total sedimentation for the intermediate lake. A distribution was then based on all simulated intermediate lake sedimentations, a lognormal distribution with geometric mean 2.82 m and geometric standard deviation 1.71, as presented in Figure 11.

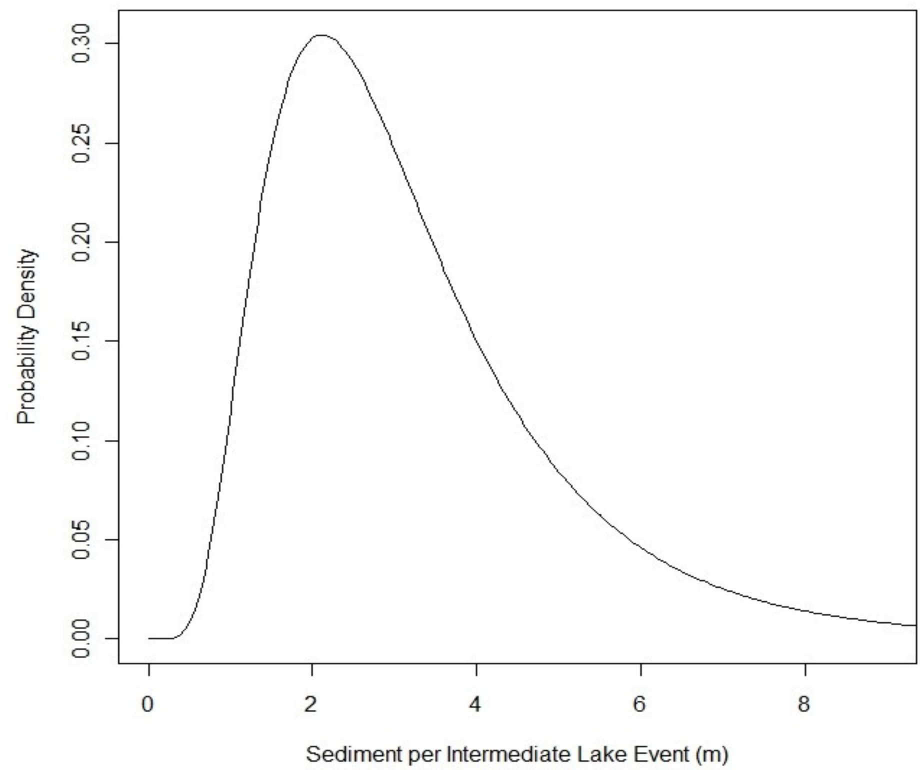


**Figure 11. Probability density function for the total sediment thickness associated with an intermediate lake (or the transgressive of regressive phase of a large lake).**

The net effect is that the sedimentation rates are on the order of 15-20 m per glacial cycle (100 ky). For the duration of the model (2.1 My), this implies sedimentation of more than 300 m. The Basin and Range system accommodates this rate of sedimentation because it is an extensional system. That is, sedimentation continues as the basins expand and subside, maintaining similar elevation in each cycle.

## 6.4 Destruction of the Waste Embankment

A scenario involving destruction of the Energy*Solutions* waste embankment was modeled. That is, intermediate lakes are assumed to be sufficiently large that wave energy from such a lake will destroy the above-ground portions of the DU waste cell. In effect, conceptually this differentiates a shallow lake from an intermediate lake. The precise elevation needed for this to happen is not considered for the model, but the intermediate lakes that occur in the model are intended to match this definition.

The first lake in the time period assessed is likely to be an intermediate lake but can be a large lake. The destruction is handled equivalently in either case, as the conceptual model treats the transgressive phase of a large lake as behaving similarly to an intermediate lake.

The mass of material that is within the embankment above the grade of the surrounding land is assumed to be dispersed by wave action. This volume of above grade material in the embankment, including DU waste, fill material and cap material, is assumed to be mixed with the sediment associated with the intermediate lake, and subsequently spread across the dispersal area. It is assumed that the volume of material below grade is simply covered by sediment (i.e., sediment that is mixed with the above-grade waste). However, the DU waste included in the below grade layers is also included in the dispersed waste. That is, the total volume dispersed is the volume above grade, but the total mass of waste dispersed is the entirety of the DU waste that is still contained in the disposal system. Including the below grade DU waste is clearly conservative, but is a simplification that has been taken in this model. Some DU waste could be emplaced below grade, and, if not, then a diffusion gradient will cause mixing with below grade sedimentary layers. That is, some DU waste will move down, but, instead, all of the DU waste still in the disposal system when a lake arrives is made available to lake-related transport processes.

A probability distribution for the area across which the embankment material is spread was developed based on an assumption that a destroyed site would be flattened by wave action. The probability distribution for the area was developed so that the area represents:

- at a minimum, an area that would be covered if the volume of the above-grade material were spread out to a height of 1 m, and
- for a geometric mean, an area that would be covered if the volume of the above-grade material were spread out to a height of 10 cm.

The exact distribution for area depends on the precise volume of the above-grade embankment at the time of destruction, but a lognormal distribution with geometric standard deviation 1.5, and geometric mean defined as above. A typical probability density function is shown in Figure 12.

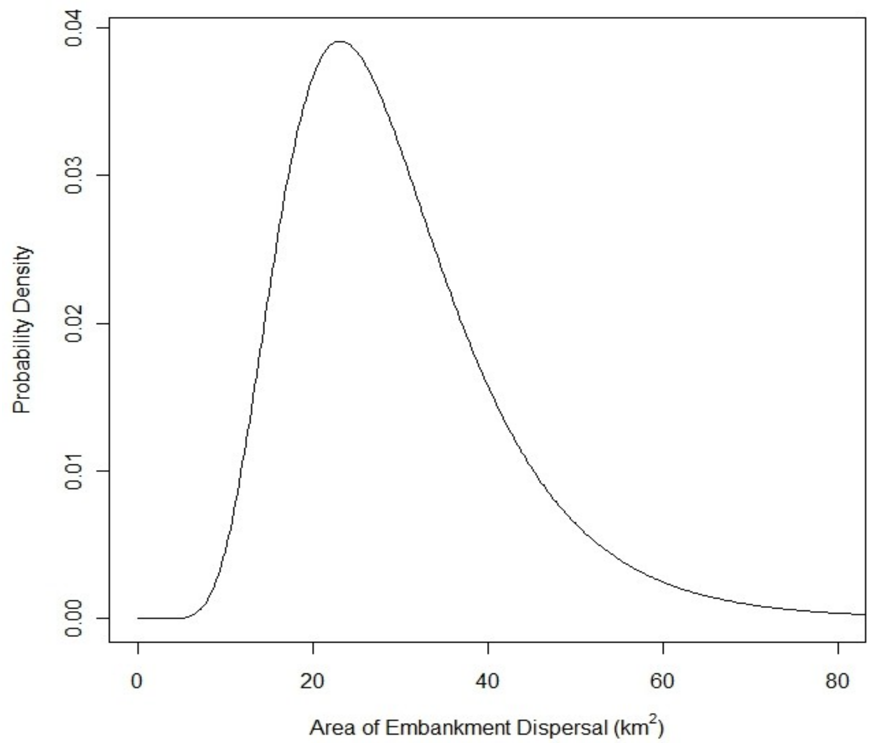


**Figure 12. Probability density function for the area over which the waste embankment is dispersed upon destruction.**

## 6.5 Reported Results

As a qualitative assessment, the deep time model does not attempt to calculate dose to human receptors, but rather to simply characterize the fate of the bulk of the waste. After the destruction of the waste embankment, the bulk of the waste will be mixed with sediments and dissolved in lake water.

Upon destruction of the waste embankment, the PA model switches modes from detailed modeling of waste transport through air dispersion, biotic uptake, groundwater flow, and other processes to a much simpler model. These processes are expected to have minor effects on transport once the waste is mixed into a sedimentary layer. The only processes that are modeled after destruction are lake recurrence, radioactive decay and ingrowth, mixing of waste with sediment, and dissolution of waste in lake water.

### 6.5.1 Concentration in Sediment

Concentration in sediment is initially calculated under the assumption that all of the waste that was above grade in the waste embankment is mixed evenly with the sediment that forms with the lake that destroys the site. Concentration in sediment is then calculated as the total radioactivity in the dispersed site divided by the volume of material into which the waste is dispersed:

$$C_{sediment} = \frac{R_{above\ grade}}{V_{material\ above\ grade} + V_{sediment}} \ . \tag{13}$$

The volume of sediment is the depth of sediment associated with the lake times the area over which the waste is dispersed.

This calculation assumes that there is no loss of waste from the initial dispersal region. While this calculation is counter to the modeling of dissolution into the water column of the lake, a simplifying assumption is that all waste that dissolves into the lake precipitates back into the sediment upon recession of the lake.

The concentrations in sediment are modeled as remaining constant, except for decay and ingrowth, until a new lake occurs. When a new lake occurs, the sedimentation associated with that lake is likely to mix with some portion of the top layer of existing sediment and leave the lower layers of the sediment buried beneath. However, for simplicity, a conservative approach is to mix all sediment that contains waste, effectively keeping some portion of the waste near-surface. The concentration is again the total radioactivity divided by the volume containing waste; however, the volume that contains waste now has the additional volume of sediment associated with the current lake.

### 6.5.2 Radioactivity in Lake Water

When lake water is present, radionuclides will partition between the water phase and the solid phase depending on element-specific solubility and sorption properties. Radionuclides remaining in the pore water will then diffuse into the lake. The waste is likely to mix over a wide area of the lake, and many forms of the waste are likely to bind with carbonate ions in the water, ultimately precipitating into carbonate sediments. As a conservative assumption, upon recession of the lake, all waste is assumed to precipitate back into the *local* sediments – meaning that all radionuclides in the sediments modeled in Section 6.5.1 are returned to the sediments when the lake regresses.

When a lake returns, the sediments are assumed to be fully saturated, and thus radionuclides are partitioned from the sediment to the pore water within the sediment using the same partitioning coefficients ($K_d$) used for other sedimentary soils in the model. An important difference between the assumptions for this model and the model for transport from the embankment in the 10 ky model is that the lake water is assigned a different solubility for uranium for the deep time assessment. While solubilities for all other radionuclides remain the same, the solubility for uranium is reduced to that of $U_3O_8$ which is significantly lower than other forms of uranium originally present in the waste. This change in solubility for uranium is adopted because it is expected that by the time the first lake returns, all soluble uranium forms ($UO_2$ and $UO_3$) will have been leached from the embankment into the shallow aquifer.

As radionuclides associated with the sediments dissolve into the pore water, they diffuse into the lake water using a constant flux model based on Fick's first law, with the following assumptions:

- There is an interface boundary layer of 0.1 m above the sediment, above which the water has a radionuclide concentration of 0. In fact, there will be some buildup of concentration as a radionuclide migrates into the water, but it will diffuse into the lake. It is conservative to assume a zero concentration, which results in the highest possible flux.

- The concentration in sediment remains constant over the deep time period. The sediment concentration should in fact diminish over time if enough mass is migrated into the water, but for simplicity, the sediment concentrations are kept constant across time steps.

The activity that is migrated to water is then:

$$R = \Delta T \cdot D_m \cdot \frac{C_V}{0.1\,\mathrm{m}} \cdot A \ , \tag{14}$$

where

- $R$ is radioactivity (Bq or pCi),
- $\Delta T$ is the time step (in s),
- $D_m$ is the diffusion coefficient ($m^2/s$),
- $C_V$ is the concentration in sediment ($Bq/m^3$ or $pCi/m^3$), and
- $A$ is the area of the sediment that contains that concentration of waste (the dispersed area, in $m^2$).

Concentration in lake water is then calculated based on the conservative assumption that the radioactive material does not dilute in a large basin of the lake but rather remains in the water column immediately above the dispersed area. That is, the concentration is calculated as:

$$C = \frac{R}{D \cdot A} \tag{15}$$

where

- $C$ is concentration (Bq/L),
- $R$ is the radioactivity (Bq),
- $A$ is the area of the sediment that contains waste (the dispersed area, in $m^2$), and
- $D$ is the depth of the lake (m).

There is an insufficient record of lake elevations to construct a data-based distribution for lake depth. Thus, the distributions for lake depth are chosen based on the conceptual model. Depths for intermediate lakes have a Beta distribution with mean 30 m, standard deviation 18 m, minimum of 0 m, and maximum of 100 m. Depths for large lakes have a Beta distribution with mean 150 m, standard deviation 20 m, minimum of 100 m, and maximum of 200 m.

For intermediate lakes, the time step is the duration of the intermediate lake. For large lakes, the lake may exist for several time steps in the GoldSim model, in which case the time step is the portion of the time step for which the lake is present. When large lakes cross multiple time steps, the concentration in sediment is allowed to change between time steps (only due to decay and ingrowth), and the activity in the lake water is accumulated over those time steps.

# 7.0 References

Archer, D. and A. Ganopolski, 2005. A movable trigger: fossil fuel $CO_2$ and the onset of the next glaciation. *Geochemistry, Geophysics, Geosystems*, 6(5), doi:10.1029/2004GC000891.

Asmerom, Y., Polyak, V. J., and S. J. Burns, 2010. Variable winter moisture in the southwestern United States linked to rapid glacial climate shifts. *Nature Geoscience*, 3, 114-117.

Berger, A., 1988. Milankovitch theory and climate. *Reviews of Geophysics*, 26(4): 624-657.

Berger, A. and M. F. Loutre, 2002. An exceptionally long interglacial ahead? *Science*, 297: 1287-1288.

Brimhall W. H. and L. B. Merritt, 1981. The geology of Utah Lake – implications for resource management. *Great Basin Naturalist Memoirs*, 5: 24-42.

Brockwell, P.J. and R.A. Davis, 1991. *Time Series: Theory and Methods*. Springer-Verlag, New York, NY.

Clark, P. U., Dyke, A. S., Shakun, J. D., Carlson, A. E., Clark, J., Wohlfarth, B., Mitrovica, J. X., Hostetler, S. W., and A. M. McCabe, 2009. The Last Glacial Maximum. *Science*, 325: 710-714.

Currey, D.R., G. Atwood, and D.R. Mabey, *Map 73 Major Levels of Great Salt Lake and Lake Bonneville*, Utah Geological and Mineral Survey, Salt Lake City, UT, May 1984

Driscoll, N. W. and G. H. Haug, 1998. A short circuit in thermohaline circulation: a cause for Northern Hemisphere glaciation. *Science*, 282: 436-438.

Einselle, G. and M. Hinderer, 1997. Terrestrial sediment yield and the lifetimes of reservoirs, lakes, and larger basins. *Geologische Rundschau*, 86: 288-310.

EPICA community members, 2004. Eight glacial cycles from an Antarctic ice core. *Nature*, 429: 623-628.

GTG (GoldSim Technology Group), 2011. *GoldSim: Monte Carlo Simulation Software for Decision and Risk Analysis*, http://www.goldsim.com

Hart, W. S., Quade, J., Madsen, D. B., Kaufmann, D. S., and C. G. Oviatt, 2004. The $^{87}Sr/^{86}Sr$ Ratios of Lacustrine Carbonates and Lake-level History of the Bonneville Paleolake System. *GSA Bulletin*, 116: 1107-1119.

Haug, G. H. and R. Tiedemann, 1998. Effect of the Formation of the Isthmus of Panama on Atlantic Ocean Thermohaline Circulation. *Nature*, 393: 673-676.

Hays, J. D., Imbire, J., and N. J. Shackleton, 1976. Variations in the Earth's Orbit: Pacemaker of the Ice Ages. *Science*, 194: 1121-1132.

Jouzel, J., Masson-Delmotte, V., Cattani, O., Dreyfus, G., *et al.*, 2007. Orbital and millennial Antarctic climate variability over the past 800,000 years. *Science*, 317: 793-796.

Kukla, G. J., R. K. Matthews, J. M. Mitchell Jr., *Quat. Res.* **2**, 261 (1972)

Lisiecki, L. E. and M. E. Raymo, 2005. A Pliocene-Pleistocene stack of 57 globally distributed benthic $\delta^{18}$O records. *Paleoceanography*, 20, PA1003, doi:10.1029/2004PA001071.

Link, P. K., Kaufmann, D. S., and Thackray, G. D., 1999. Field guide to Pleistocene lakes Thatcher and Bonneville and the Bonneville flood, southeastern Idaho, *In*: Hughes S. S. and G. D Thackray (eds.), *Guidebook to the Geology of Eastern Idaho*, Idaho Museum of Natural History, p. 251-266.

Masson-Delmotte, V., Stenni, B., Pol, K., Braconnot, P., *et al.*, 2010. EPICA Dome C record of glacial and interglacial intensities. *Quaternary Science Reviews*, 29: 113-128.

Matsurba, Y. and A. D. Howard, 2009. A spatially explicit model of runoff, evaporation, and lake extent: application to modern and late Pleistocene lakes in the Great Basin region, western United States. *Water Resources Research*, 45, W06425, doi:10.1029/2007WR005953.

Oviatt, C. G. and W. P. Nash, 1989. Late Pleistocene basaltic ash and volcanic eruptions in the Bonneville basin, Utah. *Geological Society of America Bulletin*, 101: 292-303.

Oviatt, C. G., McCoy, W. D., and Nash, W. P., 1994. Sequence stratigraphy of lacustrine deposits: a Quaternary example from the Bonneville basin, Utah. *Geological Society of America Bulletin,* 106: 133-144.

Oviatt, C. G., 1997. Lake Bonneville fluctuations and global climate change. *Geology*, 25(2): 155-158.

Oviatt, C. G., Thompson, R. S., Kauffman, D. S., Bright, J., and R. M. Forester, 1999. Reinterpretation of the Burmester core, Bonneville Basin, Utah. *Quaternary Research,* 52: 180-184.

Oviatt, C. G., D. M. Miller, J. P. McGeehin, C. Zachary, and S. Mahan, 2005. The Younger Dryas phase of Great Salt Lake, Utah, USA, *Palaeogeography, Palaeoclimatology, Palaeoecology*, 219: 263-284.

Paillard, D., 2001. Glacial cycles: toward a new paradigm. *Reviews of Geophysics*, 39(3): 325-346.

Paillard, D., 2006. What drives the Ice Age cycle? *Science*, 313: 455-456.

United States Geological Survey (USGS), 2001. National Water Information System data (Water Data for the Nation), accessed December, 2010 URL: http://waterdata.usgs.gov/

# Appendix A

## A.1 Clive Pit Wall Interpretation (C. G. Oviatt, unpublished data)

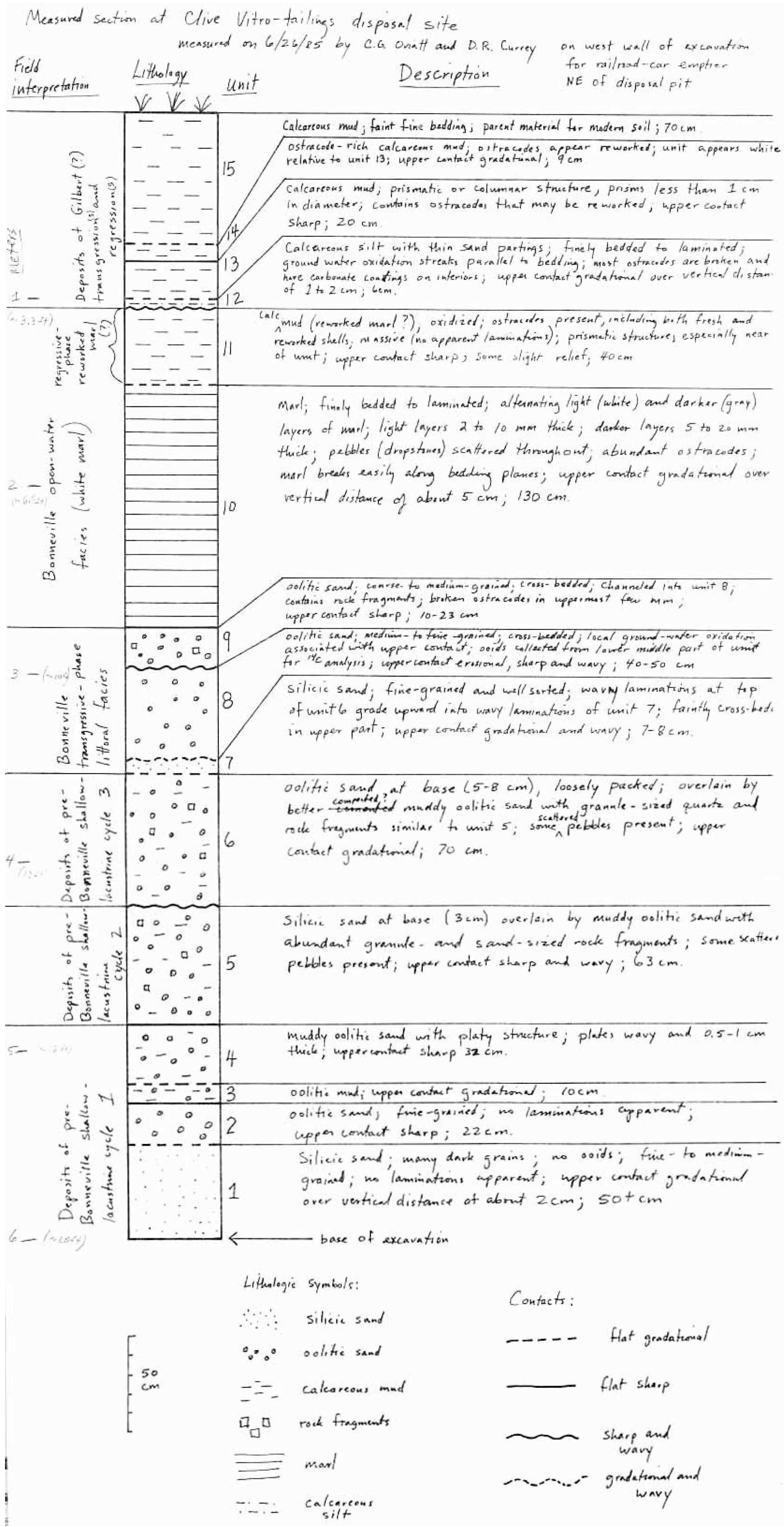
Measured section at Clive Vitro-tailings disposal site
measured on 6/26/85 by C.G. Oviatt and D.R. Currey
on west wall of excavation for railroad-car emptier NE of disposal pit
Field interpretation
Lithology
Unit
Description
Meters
Deposits of Gilbert (?) transgression(s) and regression(s)
regressive-phase reworked marl (?)
Bonneville open-water facies (white marl)
Bonneville transgressive-phase littoral facies
Deposits of pre-Bonneville shallow-lacustrine cycle 3
Deposits of pre-Bonneville shallow-lacustrine cycle 2
Deposits of pre-Bonneville shallow-lacustrine cycle 1
15
Calcareous mud; faint fine bedding; parent material for modern soil; 70 cm
ostracode-rich calcareous mud; ostracodes appear reworked; unit appears white relative to unit 13; upper contact gradational; 9 cm
14
Calcareous mud; prismatic or columnar structure, prisms less than 1 cm in diameter; contains ostracodes that may be reworked; upper contact sharp; 20 cm
13
Calcareous silt with thin sand partings; finely bedded to laminated; ground water oxidation streaks parallel to bedding; most ostracodes are broken and have carbonate coatings on interiors; upper contact gradational over vertical distance of 1 to 2 cm; 6 cm.
12
11
Calc. mud (reworked marl?), oxidized; ostracodes present, including both fresh and reworked shells; massive (no apparent laminations); prismatic structure, especially near top of unit; upper contact sharp, some slight relief; 40 cm
10
Marl; finely bedded to laminated; alternating light (white) and darker (gray) layers of marl; light layers 2 to 10 mm thick; darker layers 5 to 20 mm thick; pebbles (dropstones) scattered throughout; abundant ostracodes; marl breaks easily along bedding planes; upper contact gradational over vertical distance of about 5 cm; 130 cm.
oolitic sand; coarse- to medium-grained; cross-bedded; channeled into unit 8; contains rock fragments; broken ostracodes in uppermost few mm; upper contact sharp; 10-23 cm
9
oolitic sand; medium- to fine-grained; cross-bedded; local ground-water oxidation associated with upper contact; ooids collected from lower middle part of unit for 14C analysis; upper contact erosional, sharp and wavy; 40-50 cm
8
silicic sand; fine-grained and well sorted; wavy laminations at top of unit 6 grade upward into wavy laminations of unit 7; faintly cross-bedded in upper part; upper contact gradational and wavy; 7-8 cm.
7
6
oolitic sand at base (5-8 cm), loosely packed; overlain by better cemented? muddy oolitic sand with granule-sized quartz and rock fragments similar to unit 5; some scattered pebbles present; upper contact gradational; 70 cm.
5
Silicic sand at base (3 cm) overlain by muddy oolitic sand with abundant granule- and sand-sized rock fragments; some scattered pebbles present; upper contact sharp and wavy; 63 cm.
4
muddy oolitic sand with platy structure; plates wavy and 0.5-1 cm thick; upper contact sharp 32 cm.
3
oolitic mud; upper contact gradational; 10 cm
2
oolitic sand; fine-grained; no laminations apparent; upper contact sharp; 22 cm.
1
Silicic sand; many dark grains; no ooids; fine- to medium-grained; no laminations apparent; upper contact gradational over vertical distance of about 2 cm; 50+ cm
1
2
3
4
5
6
base of excavation
Lithologic Symbols:
silicic sand
oolitic sand
calcareous mud
rock fragments
marl
calcareous silt
50 cm
Contacts:
flat gradational
flat sharp
sharp and wavy
gradational and wavy

# Appendix B

## B.1 Knolls Core Interpretation (C. G. Oviatt, unpublished data)

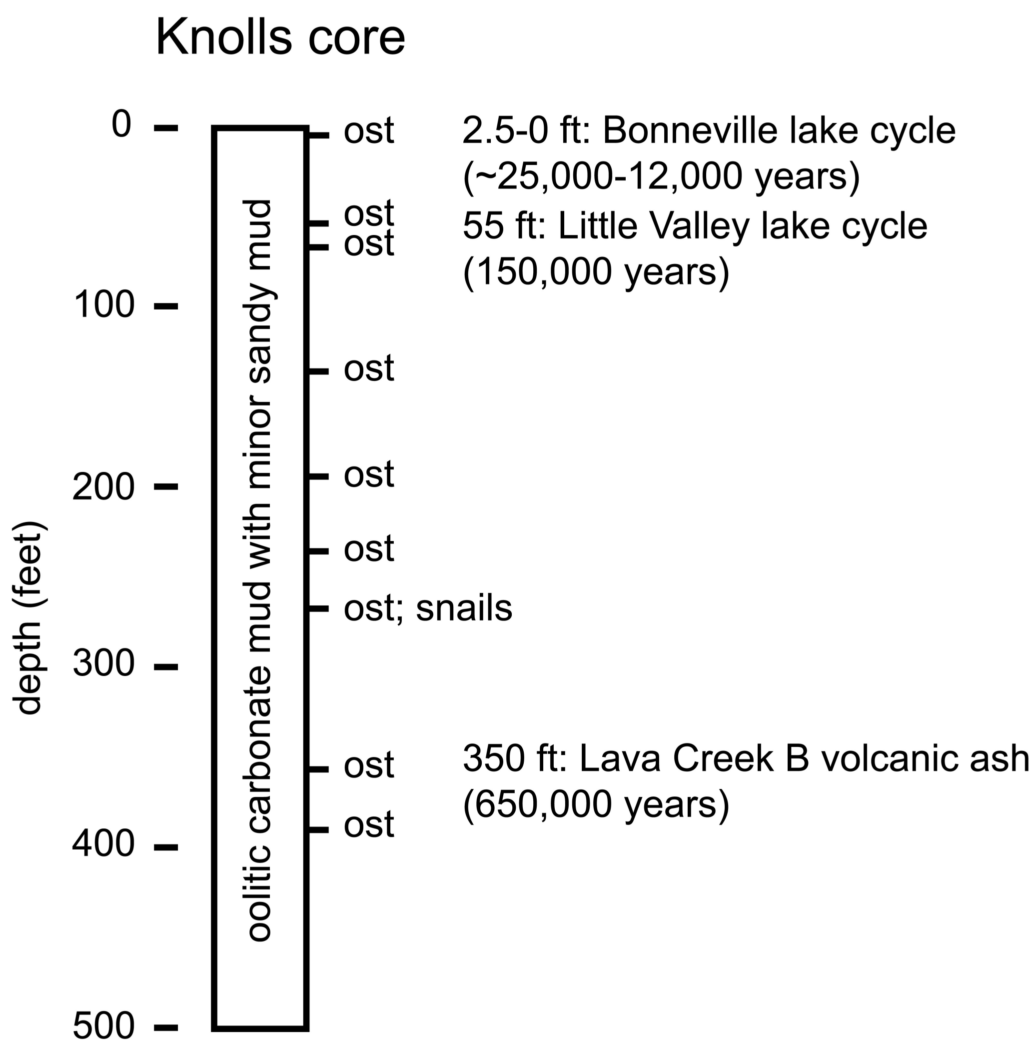


ost = ostracodes (fresh water of a lake or marsh)
snails indicate shallow fresh water